British Geological Survey
NATURAL ENVIRONMENT RESEARCH COUNCIL

Mineralogical characterisation of the Nordland Shale, UK Quadrant 16, northern North Sea

Reservoir Geoscience Programme

Commissioned Report CR/01/136

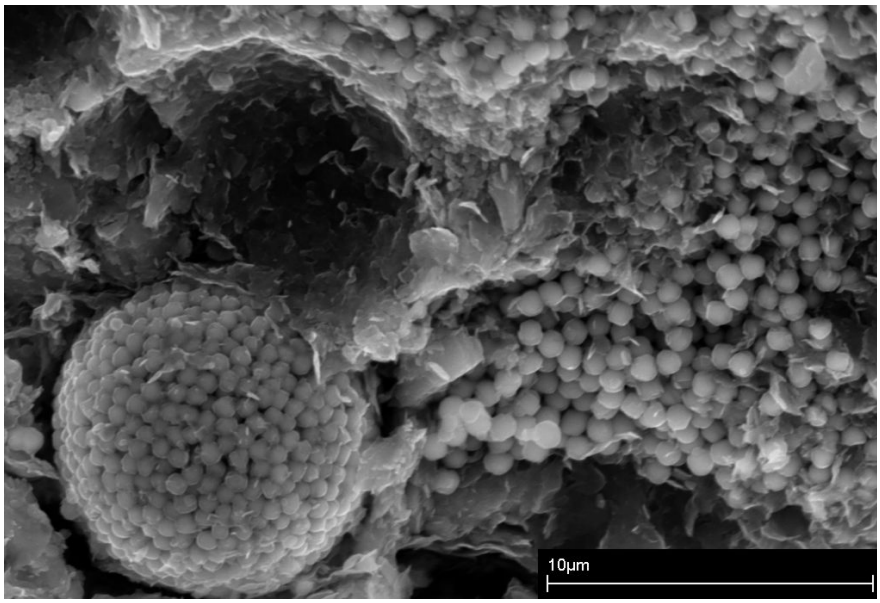

BRITISH GEOLOGICAL SURVEY

COMMISSIONED REPORT CR/01/136

Mineralogical characterisation of the Nordland Shale, UK Quadrant 16, northern North Sea

S J Kemp, J Bouch and H A Murphy

Key words

CO2 storage, Nordland Shale, North Sea, mineralogy, petrography, cap rock, clay minerals.

Front cover

Scanning electron photomicrograph of framboidal and disseminated pyrite crystals in a clay matrix.

Bibliographical reference

KEMP, S.J., BOUCH, J. AND MURPHY, H.M. 2001. Mineralogical characterisation of the Nordland Shale, UK Quadrant 16, northern North Sea. *British Geological Survey Commissioned Report*, CR/01/136. 52pp.

Keyworth, Nottingham British Geological Survey 2001

BRITISH GEOLOGICAL SURVEY

The full range of Survey publications is available from the BGS Sales Desks at Nottingham and Edinburgh; see contact details below or shop online at www.thebgs.co.uk

The London Information Office maintains a reference collection of BGS publications including maps for consultation.

The Survey publishes an annual catalogue of its maps and other publications; this catalogue is available from any of the BGS Sales Desks.

The British Geological Survey carries out the geological survey of Great Britain and Northern Ireland (the latter as an agency service for the government of Northern Ireland), and of the surrounding continental shelf, as well as its basic research projects. It also undertakes programmes of British technical aid in geology in developing countries as arranged by the Department for International Development and other agencies.

The British Geological Survey is a component body of the Natural Environment Research Council.

Keyworth, Nottingham NG12 5GG

☎ 0115-936 3241 Fax 0115-936 3488
e-mail: sales@bgs.ac.uk
www.bgs.ac.uk
Shop online at: www.thebgs.co.uk

Murchison House, West Mains Road, Edinburgh EH9 3LA

☎ 0131-667 1000 Fax 0131-668 2683
e-mail: scotsales@bgs.ac.uk

London Information Office at the Natural History Museum (Earth Galleries), Exhibition Road, South Kensington, London SW7 2DE

☎ 020-7589 4090 Fax 020-7584 8270
☎ 020-7942 5344/45 email: bgslondon@bgs.ac.uk

Forde House, Park Five Business Centre, Harrier Way, Sowton, Exeter, Devon EX2 7HU

☎ 01392-445271 Fax 01392-445371

Geological Survey of Northern Ireland, 20 College Gardens, Belfast BT9 6BS

☎ 028-9066 6595 Fax 028-9066 2835

Maclean Building, Crowmarsh Gifford, Wallingford, Oxfordshire OX10 8BB

☎ 01491-838800 Fax 01491-692345

Parent Body

Natural Environment Research Council, Polaris House, North Star Avenue, Swindon, Wiltshire SN2 1EU

☎ 01793-411500 Fax 01793-411501
www.nerc.ac.uk

Foreword

This report is the published product of a study by the British Geological Survey (BGS) and forms part of the international SACS (Saline Aquifer CO_2 Storage) project. The project aims to monitor and predict the behaviour of injected CO_2 in the Utsira Sand reservoir at the Sleipner field in the northern North Sea by methods including time-lapse geophysics, modelling its subsurface distribution and migration, and simulating likely chemical interactions with the host rock.

This report aims to provide mineralogical data to help characterise the Nordland Shale cap rock overlying the Utsira Sand reservoir.

Acknowledgements

The authors would like to thank a number of BGS colleagues who have helped to produce this report. Jonathan Pearce and Sam Holloway collected the samples and offered helpful advice. Grenville Turner is thanked for the preparation of samples for SEM analysis and Barbara Vickers for the CEC analyses.

Contents

FIGURES

PLATES

PLATES (continued)

TABLES

Summary

This report summarises the results of mineralogical and petrographic characterisation of a suite of twenty mudrock cuttings samples taken from the Nordland Shale in UK Quadrant 16, northern North Sea. A range of analyses including X-ray diffraction, scanning electron microscopy, particle-size analysis, cation exchange capacity and total organic carbon analyses were employed in order to fully characterise the samples. The results of such analyses are then used to predict the seal capacity of the Nordland Shale for injected CO_2 in the underlying Utsira Sand reservoir.

The mineralogy of the clay silts or silty clays are broadly comparable with the only previously published analyses from Norwegian Quadrant 15 and are composed of quartz, undifferentiated mica, kaolinite, K-feldspar, calcite, smectite, albite, chlorite, pyrite and gypsum together with traces of drilling mud contamination. The clay mineralogy of the Nordland Shale is generally dominated by illite with minor kaolinite and traces of chlorite and smectite. Modelling of clay mineral crystallite size distributions suggests shallow burial to perhaps <2000 m.

Petrographic analysis suggests that most of the samples are massive although some present evidence of a weak sedimentary lamination. The samples are non-organic and are classified as non-organic mudshales and mudstones according to the Krushin (1997) classification.

Composite downhole plots suggest an increasingly silty and smectitic character with depth, particularly below 3400 ft. This feature was previously noted at shallower depths in Norwegian Quadrant 15. An understanding of whether this feature represents different diagenetic processes in more porous lithologies or alternatively the greater ingress of drilling mud is necessary as the lower part of the Nordland Shale will form the primary seal with the Utsira Sand reservoir.

Although the presence of small quantities of smectite in the Nordland Shale may invalidate its predictions, XRD-determined quartz contents suggest displacement pore throat diameters of between 14.5 and 21.5 nm below 3000 ft (exceptionally 46.7 nm at 16/23-1 3160 ft) rising to between 21.5 and 39.7 nm above 3000 ft for the Nordland Shale in UK Quadrant 16 using the Krushin (1997) methodology. Such displacement pore throat diameters predict capillary entry pressures of between 2 and 5.5 MPa and are capable of trapping a CO_2 column ranging from 667 to 1833 m high. Since the Utsira Sand has a maximum thickness of c.300 m in the Sleipner area, capillary leakage of CO_2 through the top seal is unlikely to occur. However, such predictions are based on leakage through a pore network only and ignore possibly more effective pathways provided by the presence of microfractures.

Seismic data indicate that the CO_2 has reached the top of the Utsira Sand even though it is likely that there are some thin clay/silt barriers (mostly c.1 m thick, but one of which may be up to 7 m thick) within the reservoir sand. Assuming these shale barriers have a similar mineralogy and fabric to the overlying Nordland Shale and that they are present in the injection area, the CO_2 must be passing through by some ‘non-capillary’ entry method.

1 Introduction

Due to the global warming threat posed by anthropogenic greenhouse gases there is an urgent need to develop ways of lowering industrial CO_2 emissions. The world's first subsurface CO_2 sequestration operation is currently running at the Sleipner field in the northern North Sea. Here, CO_2 is being injected into the Mio-Pliocene Utsira Sand, a subsurface saline aquifer, at a depth of about 1000 m below sea level. The injected CO_2 then migrates upwards but is trapped by the overlying, shale-dominated Nordland Group. The operation commenced in 1996, and is expected to last for 20 years, injecting at an average rate of about one million tonnes per year.

The British Geological Survey (BGS) is part of the international SACS (Saline Aquifer CO_2 Storage) project, whose aims include monitoring the injected CO_2 by time-lapse geophysical methods, modelling its subsurface distribution and migration, and simulating likely chemical interactions with the host rock.

As part of this study, this report describes the mineralogical characterisation of samples of the Nordland Shale, the cap rock sequence over the Utsira Formation, northern North Sea. Prior to the SACS program, characterisation of the Nordland Shale was limited to interpretation of seismic data, wire-line logs and the macroscopic description of cuttings. As part of the SACS program, Lothe & Zweigel (1999) and Bøe & Zweigel (2000) provided quantitative mineralogical descriptions of samples from Norwegian Block 15/9 using X-ray diffraction and petrographic analyses. This report presents similar data, augmented by further analytical techniques, for samples from UK Quadrant 16, to the west of the Sleipner area. By employing the empirical relationships suggested by Krushin (1997), such mineralogical data can be used to determine the maximum CO_2 column required to cause capillary failure in the cap rock seal.

2 Samples

The twenty samples characterised in this study were sampled during 2000 from Blocks 16/08, 16/13, 16/18, 16/23, 16/28 and 16/29 in the UK sector of the South Viking Graben by S Holloway and J Pearce (BGS) from cuttings held at the DTI Core Store, Gilmerton Road, Edinburgh. The map shown in Figure 1 indicates the location of the UK Quadrant 16 with respect to the Utsira Formation, Sleipner field and Northern and Central North Sea.

The geological framework of the area was summarised by Bøe & Zweigel (2000). In summary, the cap rock sequence for the Utsira Sand varies between 200 and 300 m in thickness in the Sleipner area which can be divided into three subunits on the basis of geophysical response. The most important of these for the present study is the lower Upper Pliocene unit or 'shale drape', a 50 m thick sequence which directly overlies the Utsira Sand. Although predominantly composed of mudstone, the 'shale drape' also contains an eastward thickening sand wedge up to 25 m thick. Sand and silt stringers also occur towards the base of the middle unit, close to the basin margins (Chadwick *et al.*, 2000).

Table 1 provides depth-ordered sample information and the analytical scheme followed in each case. In order to fully characterise the samples, a range of analytical procedures were applied including X-ray diffraction (XRD) analysis of whole-rock and separated clay fractions, particle-size analysis (PSA), petrographic analysis using a scanning electron microscope to look at stub-mounted grains, total organic carbon (TOC) and cation exchange capacity (CEC) determinations. The quantity of sample available varied from >10 g to <0.2 g in some cases. Such small sample masses limited the number and type of analyses applied. For the purposes of this report, all depth intervals were converted to feet measurements.

3 Laboratory methods

3.1 GENERAL SAMPLE PREPARATION

Initially, small quantities of each sample were removed for petrographic analysis. Half of the remaining material was then subsampled and hammer-milled to <0.12 mm for whole-rock XRD analysis, TOC analysis and CEC determinations.

Table 1. Samples and analytical scheme

Well	Depth			BGS code	Analytical scheme					
	ft	Mean ft	m		SEM stub	Bulk XRD	Clay XRD	PSD	CEC	TOC
16/13-1	2050	2050	625	G427						
16/08-1	2250	2250	686	G422						
16/13-1	2650	2650	808	F669						
16/18-4	2776	2776	846	G428						
16/29-1	2975	2975	907	G413						
16/23-1	3100	3100	945	G419						
16/28-3	3117	3117	950	G416						
16/29-1	3125	3125	952	G414						
16/29-2	3125-3150	3138	956	G409						
16/23-1	3160	3160	963	F385						
16/28-3	3183	3183	970	G417						
16/28-3	3248	3248	990	G418						
16/29-1	3275	3275	998	G415						
16/29c-10	3300-3330	3315	1010	F393						
16/28-11	3347	3347	1020	G429						
16/29-4	3350-3375	3363	1025	G420						
16/29-4	3450-3475	3463	1055	G421						
16/28-5	3609	3609	1100	G410						
16/28-5	3708	3708	1130	G411						
16/28-5	3839	3839	1170	G412						

Analysis completed Insufficient material for analysis

3.2 X-RAY DIFFRACTION ANALYSIS

In order to produce a finer and uniform particle-size for whole-rock XRD analysis, a portion of the hammer-milled material was micronised under acetone for 10 minutes and dried at 55°C. The resulting dried material was disaggregated in a pestle and mortar and backloaded into a standard aluminium sample holder. Where less material was available, a reduced-capacity mount was used.

In order to determine the nature of any clay minerals present in the samples, 1 to 2 g of each sample was placed in a plastic bottle with approximately 50 ml deionised water and dispersed by shaking and treatment with ultrasound. The dispersed samples were then placed in a 250 ml measuring cylinder with 0.5 ml 0.1M sodium hexametaphosphate ('Calgon') solution to disperse the individual clay particles and prevent flocculation.

After standing for a period determined from Stokes' Law, a nominal <2 μm fraction was removed. The cylinders were then topped up with deionised water, stirred and the particles allowed to settle before extracting any remaining <2 μm material. This process was repeated until no further <2 μm material remained in the cylinders. The <2 μm ('clay') material and remaining 2-63 μm ('silt') material were then dried at 55°C and stored in glass vials. 100 mg of the dried <2 μm material was then re-dispersed in 2 ml deionised water using an ultrasonic bath and pipetted onto a ceramic tile in a vacuum apparatus to produce an oriented mount. The mounts were Ca-saturated using 2 ml of 1M $CaCl_2.6H_2O$ solution, washed twice to remove excess reagent before being allowed to dry at room temperature.

XRD analyses were carried out using a Philips PW1700 series automatic diffractometer equipped with a cobalt target X-ray tube and operating at 45 kV and 40 mA. Diffraction data were analysed using Philips X'Pert software coupled to an International Centre for Diffraction Data (ICDD) database running on a Gateway personal computer system. The whole-rock samples were scanned from 3-50 °2θ at a scanning speed of 0.48 °2θ/minute.

Following identification of the mineral species present in the samples, whole-rock mineral quantification was achieved using the Reitveld refinement technique using Siroquant v.2.5 software. This method avoids the need to produce synthetic mixtures and involves the least squares fitting of measured to calculated XRD profiles using a crystal structure databank. Errors for the quoted mineral concentrations are probably ±5% accuracy for quartz, calcite, halite, sylvite and barite. Larger errors are possible for the quoted 'mica', chlorite, smectite, kaolinite, gypsum and feldspar concentrations.

The oriented mounts were scanned from 2-32 °2θ also at 0.48 °2θ/minute after air-drying, ethylene glycol-solvation and heating to 550°C for 2 hours. Ethylene glycol-solvation was achieved by placing the samples in a desiccator filled with the reagent and heating to 55°C overnight.

In order to assess the relative proportions of any clay minerals present in the samples, modelling of their XRD profiles was carried out using Newmod-for-Windows™ (Reynolds & Reynolds, 1996) software. The modelling process requires the input of diffractometer, scan parameters and a quartz intensity factor (instrumental conditions) and the selection of different clay mineral sheet compositions and chemistries. In addition, an estimate of the crystallite size distribution of the species may be determined by comparing peak profiles of calculated diffraction profiles with experimental data. By modelling the individual clay mineral species in this way, *mineral reference intensities* were established and used for quantitative standardization following the method outlined in Moore and Reynolds (1997).

3.3 CATION EXCHANGE CAPACITY

Cation exchange capacity (CEC) determinations were carried out using 0.5 g portions of hammer-milled material and a scaled-down version of the normal $BaCl_2$/triethanolamine titration method. BGS experience has shown that this modified method appears to give a slightly increased CEC value. Data for standard materials analysed with the samples indicates that values might be increased by 10%.

3.4 TOTAL ORGANIC CARBON ANALYSIS

Total organic carbon (TOC) analyses were carried out by ALcontrol Geochem Ltd, Chester on 1 g portions of hammer-milled material. The samples were previously treated to obtain material containing only organic carbon compounds and then heated in a flow of oxygen in a Leco CS444 carbon/sulphur analyser. Any carbon present in the samples was therefore converted to carbon dioxide which was measured by an infra-red detector. The percentage carbon was then calculated with respect to the original sample weight.

3.5 PETROGRAPHIC ANALYSIS

Scanning electron microscope (SEM) analysis was conducted in order to assess micro-fabrics within the mudrocks, and to identify the mineralogical makeup of the silt and sand-grade particles. In addition, attention was paid to the presence/absence of contaminant phases.

Small rock fragments (typically 2-5 mm in diameter) were recovered from the cuttings samples, mounted on SEM stubs and carbon coated. Observations were made using a LEO 435VP variable pressure digital SEM with an Oxford Instruments ISIS300 digital energy dispersive X-ray microanalysis (EDXA) system, and a Cambridge Stereoscan S250 Mark I SEM with a Link 860 EDXA system. On both instruments an accelerating voltage of 20kV was used, and qualitative EDXA spectra were acquired to aid mineral identification based on their chemical characteristics. Images were recorded digitally on the LEO SEM and photographically on the S250 SEM.

4 Results

4.1 PARTICLE-SIZE ANALYSIS

The results of the particle-size analysis achieved during preparation of the samples for <2 μm XRD analysis are summarised in Table 2.

All of the samples fall within the clay silt or silty clay fields defined by Shepard (1954) and illustrated in Figure 2. Most of the samples lie within or very close to the boundary of the silty clay field. The four slightly coarser-grained samples are all those from well 16/28-5 (3609, 3708 and 3839 ft) and the single sample from well 16/18-4 (2776 ft).

A composite downhole plot of %sand, %silt and %clay (Figure 3) illustrates the approximately similar particle-size distribution of the samples but also highlights the slightly coarser-grained nature of the deepest samples.

4.2 X-RAY DIFFRACTION ANALYSIS

The results of whole-rock and <2 μm fraction XRD analysis are summarised in Tables 3 and 4. Example labelled whole-rock and <2 μm fraction XRD charts are reproduced in the Appendix.

Generally, the samples are predominantly composed of quartz, undifferentiated mica species ('mica', including muscovite and illite) and kaolinite with subordinate amounts of feldspar (K-feldspar and albite), calcite, smectite, chlorite, pyrite, gypsum and halite. Barite and sylvite are occasionally present but can form up to 17% sample.

A composite depth plot for the samples is shown in Figure 4. Below c.3000 ft, quartz contents are between 25 and 30% with the exception of the quartz-rich sample (48%) from 16/23-1 3160 ft. Above c.3000 ft, quartz contents generally increase to between 30 and 43%. K-feldspar

content (2-7%) is generally uniform while albite content (not detected-8%) generally decreases with increasing depth.

Table 2. Summary of particle-size analysis and classification

Well	Mean depth (ft)	%sand (>63 µm)	%silt (2-63 µm)	%clay (<2 µm)	Classification (Shepard, 1954)
16/13-1	2050	0	50	50	Clay silt/Silty clay
16/08-1	2250	3	50	47	Clay silt
16/13-1	2650	7	48	45	Clay silt
16/18-4	2776	0	58	42	Clay silt
16/29-1	2975	8	42	50	Silty clay
16/23-1	3100	5	44	51	Silty clay
16/28-3	3117	4	40	56	Silty clay
16/29-1	3125	4	42	54	Silty clay
16/29-2	3138	5	49	47	Clay silt
16/23-1	3160	4	47	50	Silty clay
16/28-3	3183	5	42	53	Silty clay
16/28-3	3248	5	45	50	Silty clay
16/29-1	3275	3	43	54	Silty clay
16/29c-10	3315	1	44	55	Silty clay
16/28-11	3347	2	41	57	Silty clay
16/29-4	3363	5	37	58	Clay silt
16/29-4	3463	4	34	62	Silty clay
16/28-5	3609	2	63	35	Clay silt
16/28-5	3708	2	61	37	Clay silt
16/28-5	3839	0	60	40	Clay silt

The distribution of phyllosilicates (including the clay minerals) generally shows uniform distributions for 'mica' (14-42%), kaolinite (6-19%) and chlorite (1-2%) through the depth interval sampled, although fluctuating contents are noted between c.3100 and 3400 ft. Smectite content is generally low above c.3100 ft (<4%) but increases at greater depths to reach 9%. 'Mica' and kaolinite are the most abundant phyllosilicates/clay minerals in the samples.

Calcite (not detected-11%), pyrite (not detected-5%) and gypsum (not detected-7%) contents show no obvious depth-related trend. However, pyrite and gypsum appear inversely correlated, perhaps reflecting the later development of gypsum from earlier-formed diagenetic pyrite.

Halite concentrations (not detected-5%) are approximately uniform for all the samples but sylvite and barite are more sporadically developed. Sylvite principally occurs in the samples from well 16/28-3 where it forms up to 9% sample but it also forms a trace component of the sample from well 16/13-1 at 2650 ft. Barite forms a significant part of samples from wells 16/23-1, 16/28-5 and 16/29-1.

Table 3. Summary of quantitative whole-rock X-ray diffraction analysis

Well	Mean depth (ft)	%mineral												
		quartz	K-feldspar	albite	calcite	'mica'	kaolinite	smectite	chlorite	pyrite	gypsum	halite	sylvite	barite
16/13-1	2050	35	6	8	4	34	6	2	2	1	nd	2	nd	nd
16/08-1	2250	29	5	4	5	28	16	2	2	nd	6	3	nd	nd
16/13-1	2650	43	6	4	2	29	9	2	1	1	nd	2	1	nd
16/18-4	2776	35	5	6	nd	30	16	4	2	nd	nd	2	nd	nd
16/29-1	2975	31	6	4	5	23	14	3	1	nd	3	2	nd	9
16/23-1	3100	27	5	3	1	28	10	1	2	1	2	3	nd	17
16/28-3	3117	31	5	4	2	28	15	2	1	1	nd	2	9	nd
16/29-1	3125	25	5	2	1	26	14	1	1	1	6	4	nd	14
16/29-2	3138	29	3	nd	2	40	12	6	1	1	2	4	nd	nd
16/23-1	3160	48	6	nd	2	14	7	2	1	1	nd	3	nd	16
16/28-3	3183	30	4	3	2	34	15	2	1	4	1	nd	4	nd
16/28-3	3248	26	3	nd	2	39	15	2	1	1	nd	2	9	nd
16/29-1	3275	23	7	nd	2	26	13	4	2	2	7	4	nd	10
16/29c-10	3315	27	4	nd	nd	42	15	9	1	2	nd	nd	nd	nd
16/28-11	3347	25	4	4	11	36	15	2	2	nd	nd	1	nd	nd
16/29-4	3363	28	3	4	3	32	18	3	2	2	nd	5	nd	nd
16/29-4	3463	26	2	3	5	35	18	3	2	2	nd	4	nd	nd
16/28-5	3609	25	5	nd	7	33	7	7	1	2	1	1	nd	11
16/28-5	3708	29	4	nd	11	16	17	5	1	2	nd	2	nd	13
16/28-5	3839	27	3	nd	3	27	19	8	1	5	nd	2	nd	5

In order to provide quantitative clay mineralogical data, peak integration was performed on the illite 002 (~5Å), kaolinite 002 (3.58Å), chlorite (3.54 Å), and smectite 005 (~3Å) reflections. These are suitable reflections as they are close together and therefore minimize geometry and sample thickness effects. Sample peak areas were then compared with those derived from modelling the individual clay mineral species with Newmod-for-Windows™ and clay concentrations produced.

Clay mineral distributions are shown in the composite plots in Figure 5. The sample's <2 μm fractions are generally dominated by illite with minor kaolinite and traces of chlorite and smectite.

Above c.3400 ft, the proportions of the different clay minerals in the <2 μm fractions is approximately similar; illite 68%, kaolinite 18%, chlorite 9% and smectite 5%. The exception to this composition being the more smectite-rich sample from 3315 ft in well 16/29c-10. However below c.3400 ft, smectite and kaolinite content increases while illite and chlorite decreases to a composition of illite 41%, kaolinite 37% and smectite 23% in the deepest sample.

Table 4. Summary of quantitative <2 µm fraction X-ray diffraction analysis

Well	Mean depth (ft)	%clay mineral			
		smectite	illite	chlorite	kaolinite
16/13-1	2050	4	72	9	15
16/08-1	2250	5	69	7	18
16/13-1	2650	8	62	9	21
16/18-4	2776	7	73	7	13
16/29-1	2975	5	66	10	19
16/23-1	3100	6	68	9	18
16/28-3	3117	5	70	8	17
16/29-1	3125	3	70	9	19
16/29-2	3138	8	64	10	18
16/23-1	3160	6	67	9	18
16/28-3	3183	5	67	9	18
16/28-3	3248	7	66	8	19
16/29-1	3275	5	69	9	18
16/29c-10	3315	19	58	6	18
16/28-11	3347	6	63	10	21
16/29-4	3363	4	69	9	19
16/29-4	3463	11	62	9	18
16/28-5	3609	15	49	9	27
16/28-5	3708	17	46	11	26
16/28-5	3839	23	41	0	37

Newmod-for-Windows™ modelling suggests that the illite in the Nordland Shale samples shows very restricted 'swelling' on glycol-solvation, exhibited by a slight sharpening of its basal XRD reflections, which may represent the presence of very few (<?2%) smectite interlayers. Modelling indicates that the illite contains 0.6 K; 0.2 Fe per $(Si, Al)_4O_{10}(OH)_2$ and typically a crystallite-size distribution with a mean defect-free distance of 7 layers and a crystallite-size range of 1 to 38 layers.

The coincidence of the kaolinite and chlorite basal XRD reflections makes accurate modelling of both species difficult. However, by careful measurement of the chlorite d_{003} and separated kaolinite d_{002} and chlorite d_{004} peaks, mean defect-free distances of 12 and 7 layers and crystallite-size ranges of 1 to 55 and 1 to 20 layers were assumed for the kaolinite and chlorite respectively. The intensity ratios for the chlorite basal XRD peaks also suggest that the chlorite present is an iron-rich variety.

The smectite identified in the samples has a mean defect-free distance of 1.5 layers and a crystallite-size range of 1 to 8 layers.

4.3 CATION EXCHANGE CAPACITY DETERMINATIONS

The CEC of mudstone samples will be chiefly determined by the quantity and types of clay mineral present. Typical values for standard clay minerals include smectite 79-112 milliequivalents per 100g, illite 27 meq/100g and kaolinite 1.9-3.3 meq/100g (van Olphen &

Fripiat, 1979). Using these standard values together with average %clay concentrations from XRD analyses and an average clay content of 54%, a typical CEC value for the Nordland Shale samples is predicted to be 16 meq/100g.

The results of CEC determinations are shown in Table 5 and the composite downhole plot (Figure 6). Values are generally within the range 15.0 to 20.2 meq/100g, close to that predicted, with the exception of the samples from 16/08-1 2250 ft and 16/29-1 3125 ft which produced values of <6.0 meq/100g. Both of these samples contain elevated gypsum concentrations (6%) which is known from previous analyses to interfere with CEC measurement by this method. The remaining samples all contain <1% gypsum.

4.4 TOTAL ORGANIC CARBON ANALYSIS

The results of TOC determinations are also shown in Table 5 and the composite downhole plot (Figure 6). Percentage TOC values are low for all the samples analysed with values ranging from 0.68 to 1.58%.

Table 5. Summary of CEC and TOC determinations

Well	Mean depth (ft)	CEC (meq/100 g)	TOC (%)
16/08-1	2250	<6.0	1.19
16/28-3	3117	15.3	0.68
16/29-1	3125	<6.0	1.58
16/29-2	3138	16.7	0.70
16/28-3	3183	15.0	1.16
16/28-3	3248	20.2	1.28
16/29-4	3363	17.2	0.74
16/29-4	3463	18.9	0.72

4.5 PETROGRAPHIC ANALYSIS

Summary descriptions for each sample are given in Table 6, and the samples are summarised below in terms of their generalised characteristics.

4.5.1 Lamination and fabric

The majority of samples (9 out of 14) have massive fabrics, with no clear lamination defined at low magnifications (Plates 1, 2 and 3). Samples 16/08-1 2250 ft, 16/23-1 3100 ft, 16/28-3 3183 ft, 16/29-1 3275 ft and 16/29-4 3463 ft, however, all contain some degree of lamination defined by the preferred orientation of clay particles (Plates 4, 5 and 6). One sample (16/28-5 3609 ft) contains well developed slickensides (Plate 7).

4.5.2 Grain/particle size and mineralogical makeup

SEM analysis confirms the results of the particle size analysis (see Section 4.1), indicating that the samples predominantly comprise sub-equal amounts of clay and silt-grade material (typically c.40-50% of each; see Table 6), with minor amounts of very fine sand-grade granular material (typically <5%).

It is apparent from Plates 3 and 6 that clay mineral particles show considerable variation in size, ranging from <2 μm to >20 μm in diameter. Therefore, the clay-grade and the silt-grade size fractions are both largely made up of clay minerals. Silt and fine sand grade material is evident in many samples, and predominantly comprises quartz and K-feldspar (Plate 8), with some rare bioclastic debris (predominantly siliceous sponge spicule fragments; Plate 9), and rarer mica noted in sample 16/28-3 3117 ft. In addition, some samples contain large voids at the sample surface, which are interpreted to represent the plucking of coarser grade grains during sample preparation (Plates 2 and 4).

Diagenetic overprinting is difficult to assess in mudrocks, however, the following features are evident:

- some clay particles display marginal development of fibrous outgrowths, which may represent authigenic illite, and some more tabular/platey crystals that may be ?kaolinite/chlorite (Plate 10).
- framboidal and disseminated pyrite is present in sample G414S1 (Plate 11).
- there is rare evidence for illitisation of detrital feldspar (Plate 12).

4.5.3 Porosity

All the samples are only very poorly porous and contain limited volumes of microporosity, which occurs between typically tightly packed clay particles. These micropores constitute only a few percent of the total rock volume, are c.1 μm in diameter and are poorly connected to each other (Plates 3, 6, 8, and 12). However, variations in the size and abundance of micropores are locally evident, as displayed by the relatively porous fabric shown in Plate 10. In addition, rare microfractures are evident (Plate 13). These features are considered to represent shrinkage cracks, induced by drying out of the sample.

4.5.4 Contamination.

The majority of samples are apparently free of contamination. However halite and/or sylvite are noted in some samples (see Table 6; Plate 14), probably representing precipitation from a combination of the formation fluid, drilling fluid and/or later contamination. In addition very rare particles of barite are present in samples 16/29-1 2975 ft and 16/23-1 3100 ft, which probably represent weighting ingredients from the drilling mud.

Table 6. Summary SEM descriptions for all analysed samples.

Well Mean depth (ft)	Fabric	Particle Size Clay Silt Sand	Mineralogy	Porosity	Contamination
16/08-1 2250 ft	Laminated.	60-65% 35-40% <1%	Predominantly quartz, with some feldspar and a single bioclast. EDXA confirms XRD clay mineralogy.	Minor micropores (μm scale) between clay particles.	One of the fragments on this stub is extensively halite contaminated.
16/29-1 2975 ft	None evident.	45-50% 45-50% c.5%	Well rounded grains of quartz up to fine sand grade. Rarer K-feldspar. Numerous voids at sample surface may represent plucked grains.	Porosity within the sample is restricted to small micropores, between relatively tightly packed clay-fabric. Minor fractures probably represent shrinkage cracks.	Minor barite.
16/23-1 3100 ft	Laminated.	50-60% 40-50% c.5%	Predominantly well rounded grains of quartz up to fine-sand-grade, rare barite (contamination), and K-feldspar.	Possible microfracture hosts some porosity. In addition, the clay-dominated matrix is locally relatively loosely packed, and moderate amounts of micropores (<1 μm) are evident.	Minor barite. The surface of one fragments is covered with rock flour/dust.
16/28-3 3117 ft	None evident.	40-50% 50-60% <5%	Some silt-grade clay particles, rigid grains are predominantly quartz, with some K-feldspar and some mica. A possible calcite grain is also noted	Negligible. Clay particles are tightly packed with no significant micropores between particles.	Some halite contamination on sample surface, but it is not possible to determine how far this extends into the sample.
16/29-1 3125 ft	None evident.	50-60% 40-50% c.2%	Fine-sand-grade quartz, and subordinate K-feldspar noted. Rare authigenic pyrite (framboids and disseminated) is present.	Minor microporosity between clay particles (less than in 16/23-1 3100 ft, and more than in 16/28-3 3117 ft).	Very minor halite.
16/29-2 3138 ft	None evident.	45-50% 45-50% c.1%	K-feldspar and quartz. The clay is much the same as seen elsewhere and comprises clay-grade to silt-grade particles and platelets.	Minor to moderate amounts of microporosity (comparable to 16/29-1 3125 ft). The clay is moderately packed, with some micropores between particles. These micropores are locally relatively abundant and large, forming voids of c.2-3 μm in diameter.	None noted.
16/28-3 3183 ft	Laminated, locally clearly defined.	45-50% 45-50% c.5%	Quartz, K-feldspar and clay particles/aggregates.	Very minor microporosity between relatively tightly packed clay particles. These micropores are c.1 μm diameter and very poorly connected. Some shrinkage cracks are noted.	None noted.
16/28-3 3248 ft	None evident.	45-50% 45-50% c.5%	Predominantly K-feldspar in coarse silt to sand grades and some quartz. Many "clay" particles are >2 μm diameter. Relatively large number of voids due to plucking of fine sand grains.	Negligible. Clay particles are tightly packed.	Widespread sylvite and minor halite.

Table 6. Summary SEM descriptions for all analysed samples (continued).

Well Mean depth (ft)	Lamination/ Fabric	Particle Size Clay Silt Sand	Mineralogy	Porosity	Contamination
16/29-1 3275 ft	Laminated.	40-45% 50-55% c.5%	Predominantly quartz in coarse silt/fine sand fraction. Many clay particles are silt grade.	Minor-to-moderate microporosity.	None noted.
16/29-4 3363 ft	A cluster of large plucked cavities may infer the presence of a sand-rich lamina.	45-50% 45-50% c.5%	Feldspar, quartz.	Very minor microporosity between clay particles. Two large ambiguous holes noted.	None Noted.
16/29-4 3463 ft	Laminated.	45-50% 45-50% c.5%	Quartz and K-feldspar, with relatively minor amounts of coarser grains. Much of the silt-grade material is clay particles which are >2 μm diameter.	Relatively abundant and large (c. 2-10 μm) micropores between clay particles. Some large, elongate pores/holes are noted.	None Noted.
16/28-5 3609 ft	No lamination. Slickensides noted in one fragment.	45-50% 50-55% c.5%	Quartz, sponge spicules and silt-grade clay particles.	Moderately microporous but with micropores heterogeneously distributed.	Significant halite on surface of one chip.
16/28-5 3708 ft	None noted.	45-50% 50-55% c.5%	Clay particles are relatively coarsely crystalline compared with other samples. Most granular material comprises quartz, feldspar and sponge spicules.	Clay appears to be randomly oriented, and locally relatively loosely packed, leading to locally high volumes of microporosity.	Patchy, but abundant halite.
16/28-5 3839 ft	None noted.	45-50% 50-55% c.5%	Some spicule fragments, quartz, K-feldspar, muscovite and silt-grade clay particles.	Microporosity between clay particles moderately abundant and large.	None noted.

5 Discussion

The mineralogy of the samples in the present study is broadly comparable with the only previously published analyses from the Nordland Shale (Lothe & Zweigel, 1999 and Bøe & Zweigel, 2000). The samples are typically clay silts or silty clays with an average composition of quartz (30%), undifferentiated mica (30%), kaolinite (14%), K-feldspar (5%), calcite (4%), smectite (4%), albite (2%), chlorite (1%), pyrite (1%), gypsum (1%). Petrographic analysis indicates that the barite (4%), halite (2%) and sylvite (1%) detected in some of the samples are almost certainly derived from drilling fluid contamination. Although they were described as uncertain trace phases, no evidence was obtained for the presence of siderite, dolomite, amphibole or zeolite identified by Bøe & Zweigel (2000).

The clay mineralogy of the samples is generally dominated by illite with minor kaolinite and traces of chlorite and smectite. Above c.3400 ft, the proportions of the different clay minerals in

the <2 μm fractions is approximately similar; illite 68%, kaolinite 18%, chlorite 9% and smectite 5%. However below c.3400 ft, smectite and kaolinite content increases while illite and chlorite decreases to a composition of illite 41%, kaolinite 37% and smectite 23% in the deepest sample. The nature of the clay mineral assemblage and their relatively small crystallite size distributions obtained from Newmod-modelling suggests that they have only reached the Early Diagenetic grade of maturity (Merriman & Kemp, 1996) and burial depths of perhaps 1-2 km. CEC values of 15.0 to 20.2 meq/100g are close to that predicted from the XRD mineralogy and particle-size determinations.

Scanning electron microscopy suggests that most of the samples are massive although some present evidence of an oriented clay mineral fabric suggesting a weak sedimentary lamination. The clay and silt fractions of the samples are dominated by clay minerals and detrital phyllosilicates while the small proportions of fine sand grade material are predominantly composed of quartz and K-feldspar with some rare bioclastic debris. The samples are typically poorly porous with only limited volumes of microporosity observed. However, variations in the size and abundance of micropores and microfractures are locally evident. The lack of porosity and evidence of diagenetic processes such as clay mineral and pyrite authigenesis and illitization of detrital feldspar suggest that the Nordland Shale has undergone moderate burial. The predominant clay fabric with limited grain support most closely resembles the type "A" or "B" seals illustrated in Sneider *et al.* (1997). These authors predicted that such seals could support a >150 m column of 35˚ API oil.

On the basis of their silt content (mean c.47%), the samples can therefore be termed 'mudshales' where laminated or 'mudstones' where massive according to the classification of Lundegaard & Samuels (1980). Together with the low TOC values (0.68 to 1.58%) obtained, the samples can be further classified as non-organic mudshales and mudstones according to the Krushin (1997) classification.

The composite downhole plots of this study suggest that the mineralogy of the Nordland Shale in UK Quadrant 16 is generally uniform but shows an increasingly smectitic character with depth, particularly below 3400 ft. Bøe & Zweigel (2000) detected a similar distribution in well N 15/9-9 with an increasing smectite content beneath a shallower depth of 675 m (2215 ft). Simplistically, this may indicate a greater (perhaps 1200 ft) depth of burial for the Nordland Shale in Quadrant 16 than Norwegian Quadrant 15.

Characterisation of the mineralogy close to the base of the Nordland Shale is of greater importance to the SACS study as this will form the interface with the injected CO_2 Utsira Sand reservoir. It is therefore interesting to note the correlation between increasing silt and smectite contents in the lower part of the Nordland Shale, which may reflect different diagenetic processes in more porous lithologies or alternatively the greater ingress of drilling mud.

Krushin (1997) suggested it is possible to predict the seal capacity of a non-smectitic, non-organic shale from its displacement pore throat diameter which in turn is related to its mineralogy and in particular its quartz content. In a study of mature Precambrian- to Jurassic-aged shales, he found that greater quartz contents produced larger pore throat sizes (assumed for this study to be diameters) and therefore lower seal capacities. By employing his equation:

$$displacement\ pore\,throat\ diameter\,(nm) = 1.4\,(\%quartz\,in\,matrix) - 20.5$$

XRD-determined quartz contents for the present study suggest displacement pore throat diameters of between 14.5 and 21.5 nm below 3000 ft (exceptionally 46.7 nm at 16/23-1 3160 ft) rising to between 21.5 and 39.7 nm above 3000 ft. However, since the largest pore throats measured in smectite-rich shales are regarded as drying-artefacts, Krushin (1997) was unable to validate his relationship between displacement pore throat diameter and quartz content by

mercury injection porosimetry (MIP) for more immature shales. Although the Nordland Shale samples of the present study are essentially non-organic (0.68 to 1.58% TOC), they contain up to 9% smectite, particular at depths below 3500 ft. It is therefore questionable whether such 'trace amounts' of smectite render the Krushin (1997) method of seal capacity determination inapplicable to the Nordland Shale.

Using the simplifications of Lindberg (1997), it is then possible to relate the displacement pore throat radius (r in nm) to the required pressure difference (Δp in MPa) for CO_2 to enter a water wet shale pore where σ (in mN/m) is the surface tension between water and CO_2:

$$\Delta p = \frac{2\sigma}{r}$$

Assuming the surface tension of CO_2 to be as low as 20 mN/m, as it is likely to be close to its critical point in the case of the Sleipner injection, and a range of displacement pore throat radii from 7.25 to 20 nm, a range of capillary entry pressures of 2 to 5.5 MPa is predicted.

According to Bøe & Zweigel (2000), the density difference between CO_2 and water at reservoir conditions of c.300 kg/m^3 creates a buoyancy pressure of 0.003 MPa for a 1 m thick CO_2 column. Therefore, the predicted capillary entry pressures suggest that the Nordland Shale in UK Quadrant 16 is capable of trapping a CO_2 column ranging from 667 to 1833 m high. Since the Utsira Sand has a maximum thickness of c.300 m in the Sleipner area, capillary leakage through the Nordland Shale would appear unlikely. Bøe & Zweigel (2000) obtained similar results for the Nordland Shale in Norwegian Quadrant 15, predicting that a 860 m high CO_2 column could be trapped and that cap rock capillary leakage was unlikely to occur.

However, seismic data indicate that the Sleipner injected CO_2 has reached the top of the Utsira Sand even though it is likely that there are some thin clay/silt barriers (mostly c.1 m thick, but one of which may be up to 7 m thick) within the reservoir sand. Assuming these shale barriers have a similar mineralogy and fabric to the overlying Nordland Shale and that they are present in the injection area, the CO_2 must therefore be passing through the shales by some ‘non-capillary’ entry method.

6 Conclusions

- The mineralogy of the samples from the Nordland Shale, UK Quadrant 16 is broadly comparable with the only previously published analyses from Norwegian Quadrant 15. The samples are typically clay silts or silty clays with an average composition of quartz (30%), undifferentiated mica (30%), kaolinite (14%), K-feldspar (5%), calcite (4%), smectite (4%), albite (2%), chlorite (1%), pyrite (1%), gypsum (1%). Petrographic analysis indicates that the barite (4%), halite (2%) and sylvite (1%) detected in some of the samples are almost certainly derived from drilling fluid contamination.
- The clay mineralogy of the Nordland Shale is generally dominated by illite with minor kaolinite and traces of chlorite and smectite. Modelling suggests shallow burial to perhaps <2000 m.
- Petrographic analysis also suggests that most of the samples are massive although some present evidence of an oriented clay mineral fabric suggesting the presence of a weak sedimentary lamination. The clay and silt fractions of the samples are dominated by clay minerals and detrital phyllosilicates while the small proportions of fine sand grade material are predominantly composed of quartz and K-feldspar with some rare bioclastic debris.
- The samples are non-organic (0.68 to 1.58% TOC), have CEC values of c.18 meq/100g and can be classified as non-organic mudshales and mudstones according to the Krushin (1997) classification.
- Composite downhole plots suggest a generally uniform mineralogy for the Nordland Shale but an increasingly silty and smectitic character is noted with depth, particularly below 3400 ft. This feature was previously noted at shallower depths in Norwegian Quadrant 15. An understanding of whether this feature represents different diagenetic processes in more porous lithologies or alternatively the greater ingress of drilling mud is necessary as the lower part of the Nordland Shale will form the primary seal with the Utsira Sand reservoir.
- Although the presence of small quantities of smectite in the Nordland Shale may invalidate its predictions, XRD-determined quartz contents suggest displacement pore throat diameters of between 14.5 and 21.5 nm below 3000 ft (exceptionally 46.7 nm at 16/23-1 3160 ft) rising to between 21.5 and 39.7 nm above 3000 ft for the Nordland Shale in UK Quadrant 16 using the Krushin (1997) methodology. Such displacement pore throat diameters predict capillary entry pressures of between 2 and 5.5 MPa and are capable of trapping a CO_2 column ranging from 667 to 1833 m high. Since the Utsira Sand has a maximum thickness of c.300 m in the Sleipner area, capillary leakage of CO_2 through the top seal is unlikely to occur. However, such predictions are based on leakage through a pore network only and ignore possibly more effective pathways provided by the presence of microfractures.
- The seismic data indicate that the CO_2 has reached the top of the Utsira Sand even though it is likely that there are some thin clay/silt barriers (mostly c.1 m thick, but one of which may be up to 7 m thick) within the reservoir sand. Assuming these shale barriers have a similar mineralogy and fabric to the overlying Nordland Shale and that they are present in the injection area, the CO_2 must be passing through by some ‘non-capillary’ entry method.

References

Most of the references listed below are held in the Library of the British Geological Survey at Keyworth, Nottingham. Copies of the references may be purchased from the Library subject to the current copyright legislation.

BØE, R, and ZWEIGEL, P. 2001. Characterisation of the Nordland Shale in the Sleipner area by XRD analysis - A contribution to the Saline Aquifer CO2 Storage (SACS) project. *SINTEF Petroleum Research Report No. 33.0764.00/01/01*

CHADWICK, R A, HOLLOWAY, S, KIRBY, G A, GREGERSON, U and JOHANNESSEN, P N. 2000. The Utsira Sand, Central North Sea – an assessment of its potential for regional CO2 disposal. *Proceedings of the 5th International Conference on Greenhouse Gas Control Technologies (GHGT-5)*, Cairns, Australia, 349 – 354.

KRUSHIN, J T. 1997. Seal capacity of nonsmectite shale. 31-47 in *Seals, Traps and the Petroleum System*. SURDAM, R C (editor). AAPG Memoir 67.

LINDEBERG, E. 1997. Escape of CO_2 from aquifers. *Energy Convers. Mgmt.*, 38, Supp., S235-S240.

LOTHE, A E, and ZWEIGEL, P. 1999. Saline Aquifer CO2 Storage (SACS). Informal annual report 1999 of SINTEF Petroleum Research's results in work area 1 'Reservoir Geology'. *SINTEF Petroleum Research Report No. 23.4300.00/03/99*

LUNDEGARD, P M and SAMUELS, N D. 1980. Field classification of fine-grained sedimentary rocks. *Journal of Sedimentary Petrology*, 50, 781-786.

MERRIMAN, R J and KEMP, S J. 1996. Clay minerals and sedimentary basin maturity. *Mineralogical Society Bulletin*, 111, 7-8.

MOORE, D M and REYNOLDS, R C. 1997. *X-Ray Diffraction and the Identification and Analysis of Clay Minerals*, Second Edition. Oxford University Press, New York.

REYNOLDS, R C and REYNOLDS, R C. 1996. *Description of Newmod-for-Windows™. The calculation of one-dimensional X-ray diffraction patterns of mixed layered clay minerals*. R C Reynolds, 8 Brook Road, Hanover, NH 03755, USA.

SHEPARD, F P. 1954. Nomenclature based on sand-silt-clay ratios. *Journal of Sedimentary Petrology*, 24, 151-158.

SNEIDER, R M, SNEIDER, J S, BOLGER, G W and NEASHAM, J W. 1997. Comparison of seal capacity determinations: conventional cores vs. cuttings. 1-12 in *Seals, traps, and the petroleum system*. SURDAM, R C. (editor). AAPG Memoir 67.

VAN OLPHEN, H and FRIPIAT, J J. 1979. *Data handbook for Clay Materials and other Non-Metallic Minerals*. Pergamon Press.

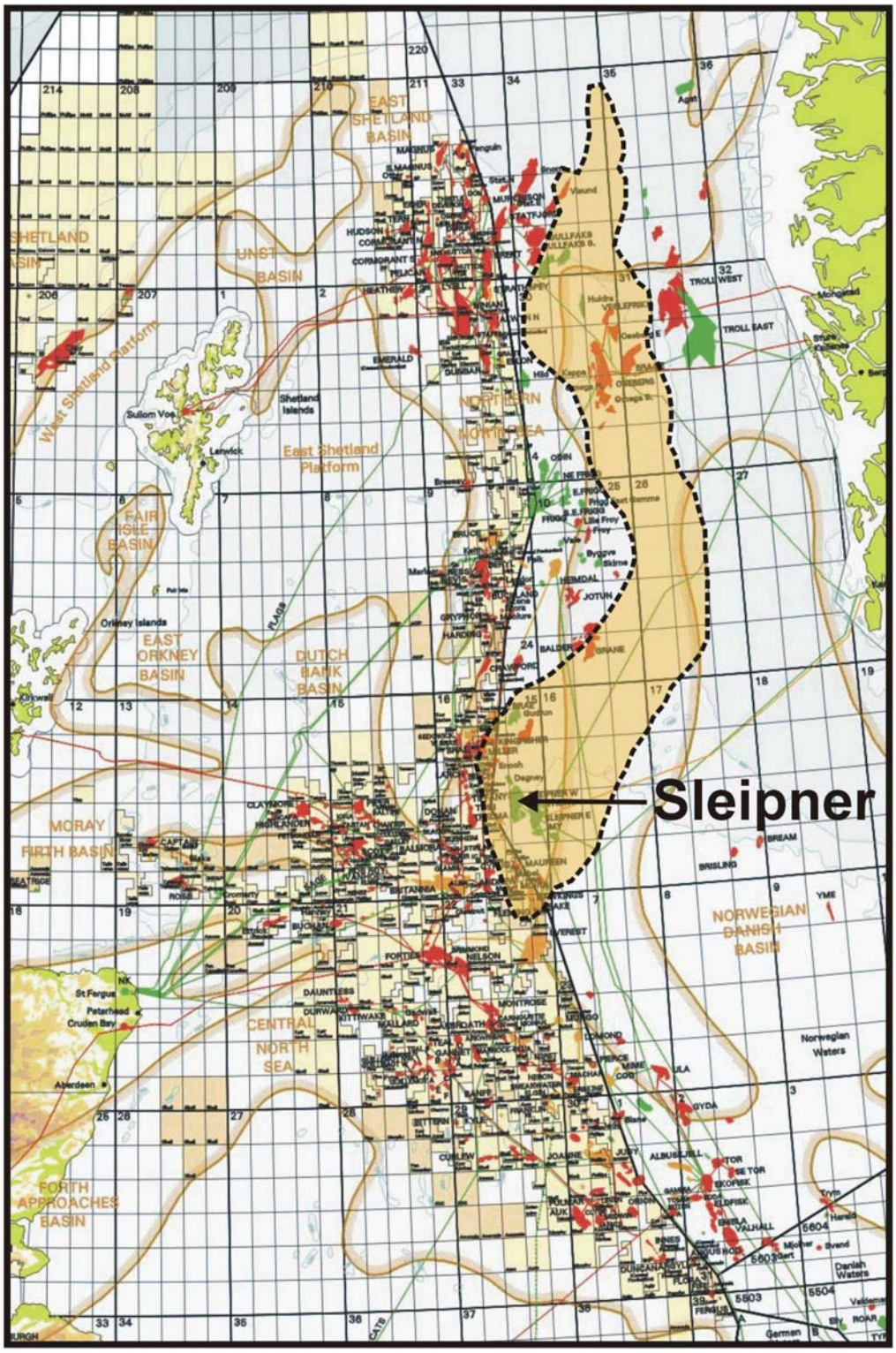

Figure 1. Northern and Central North Sea map showing location of Utsira Formation, Sleipner field and UK Quadrant 16 (just west of Sleipner).

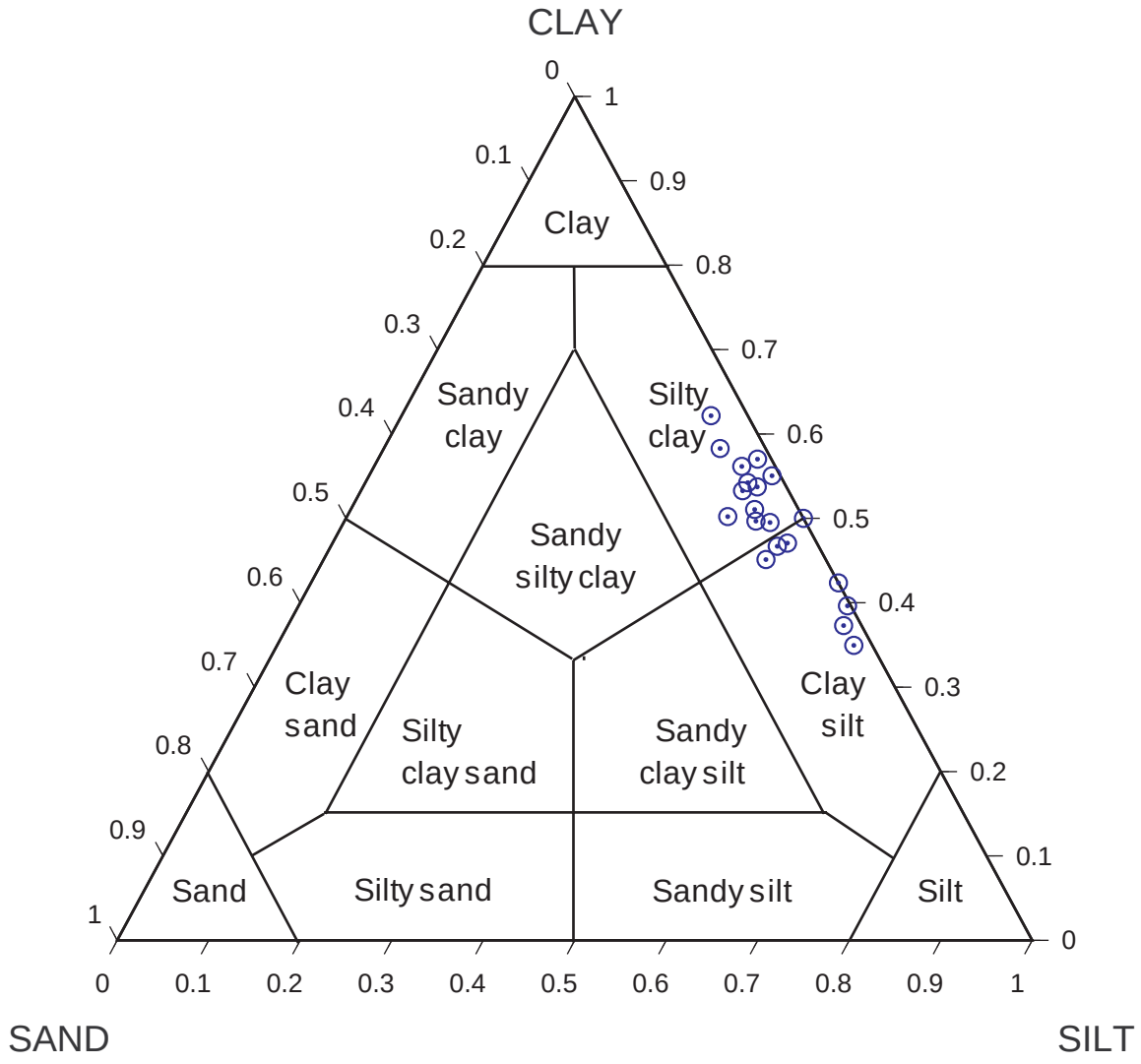

Figure 2. Triangular plot of particle-size data (after Shepard, 1954)

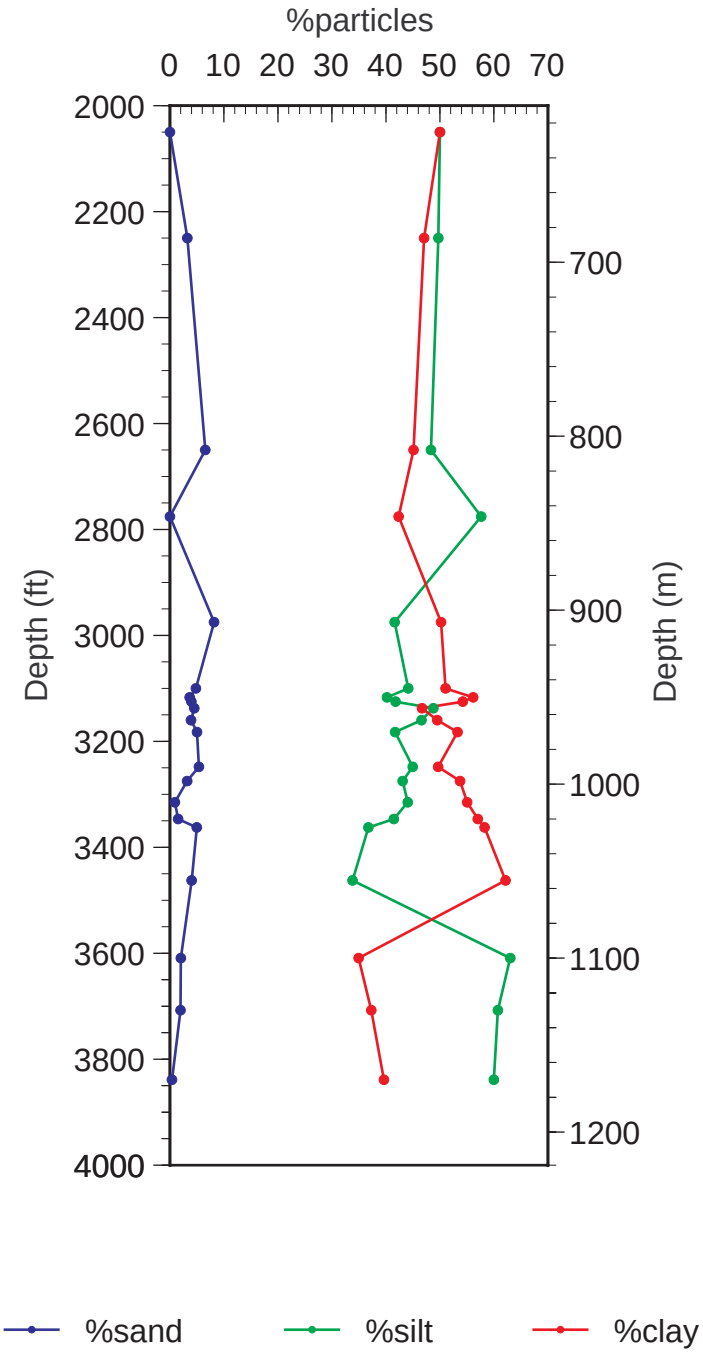

Figure 3. Downhole composite plot of particle-size distributions

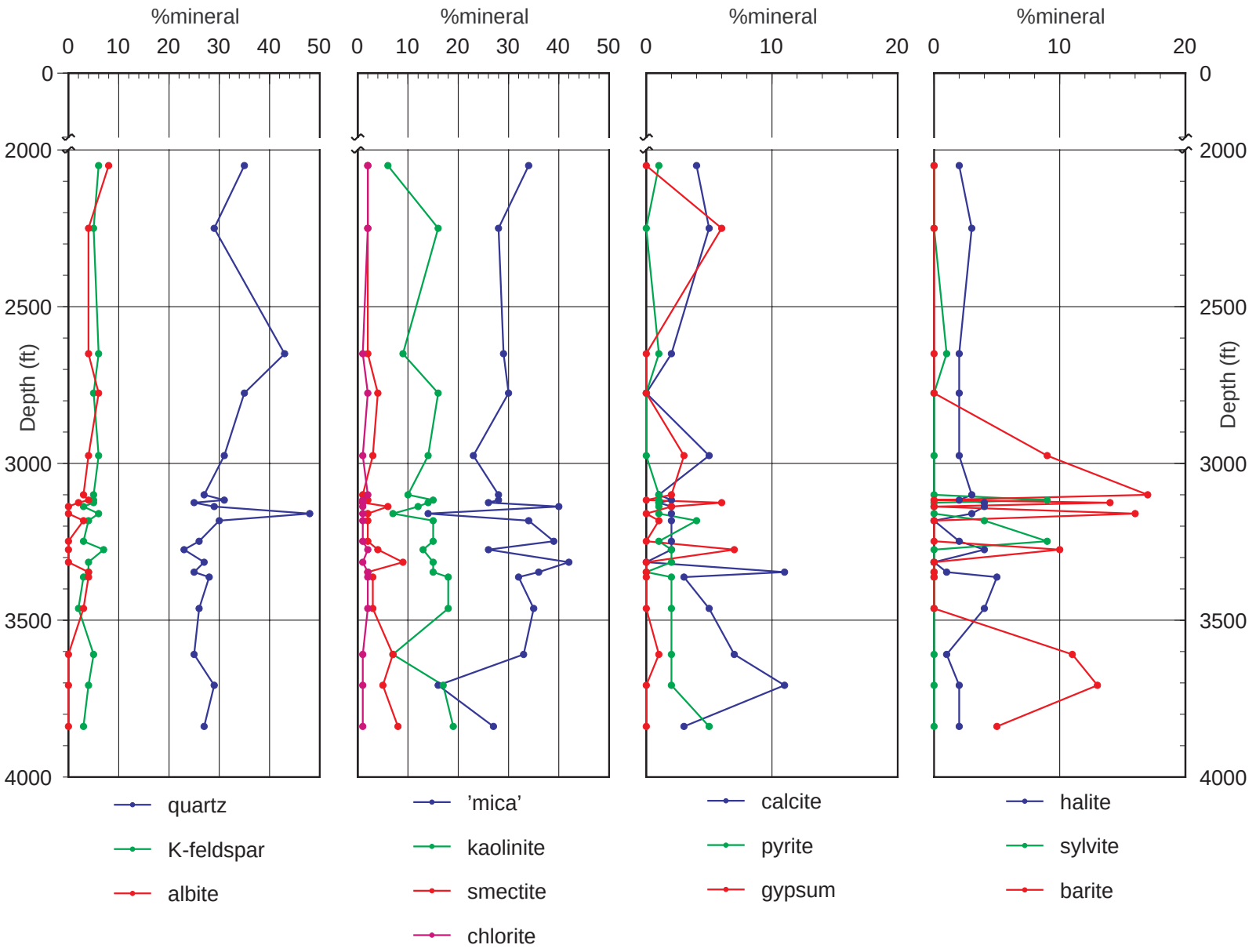

Figure 4. Downhole composite plots of whole-rock composition

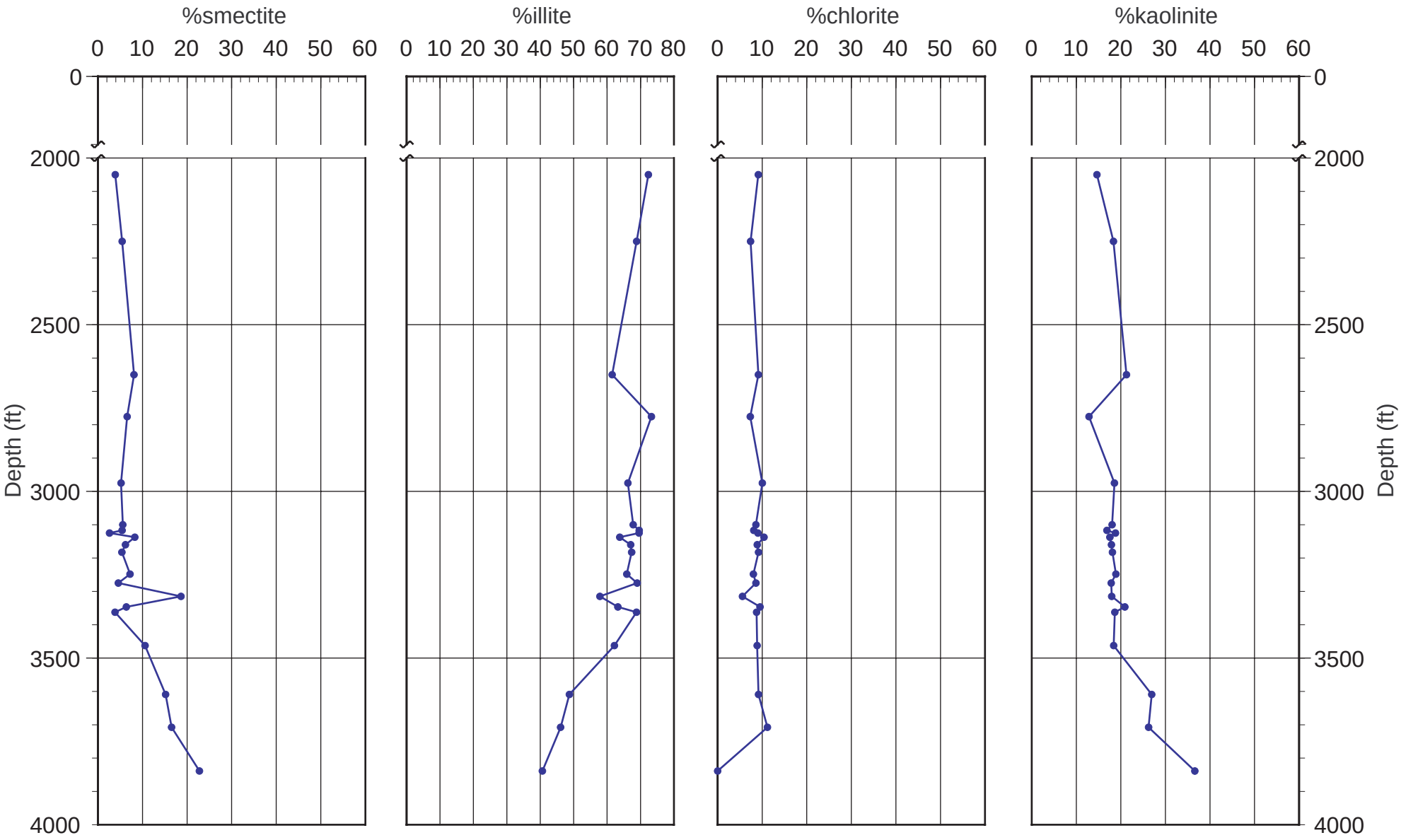

Figure 5. Downhole composite plot of clay mineral distribution

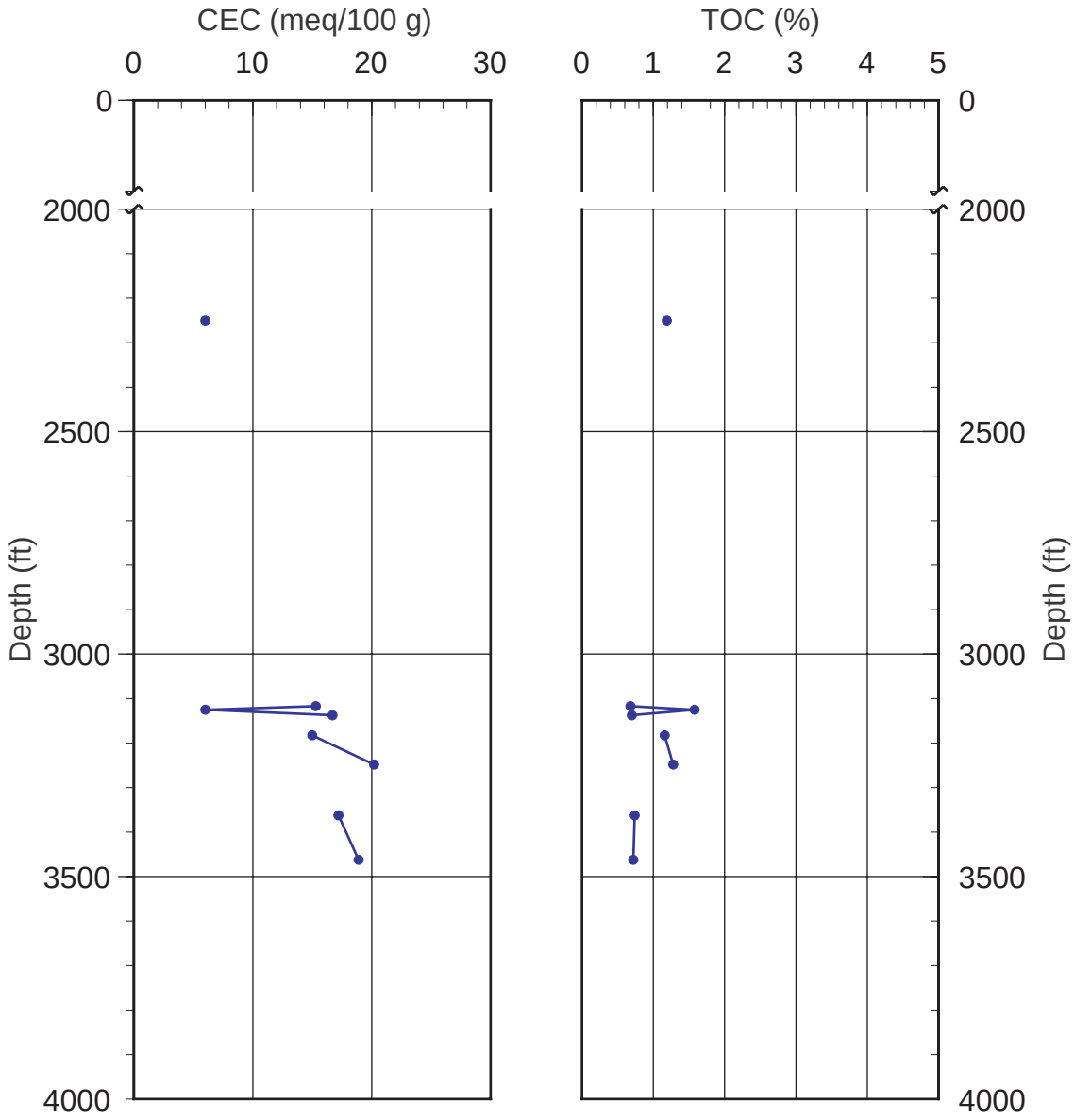

Figure 6. Downhole composite plots of cation exchange capacity and total organic carbon content.

MASSIVE MUDROCKS

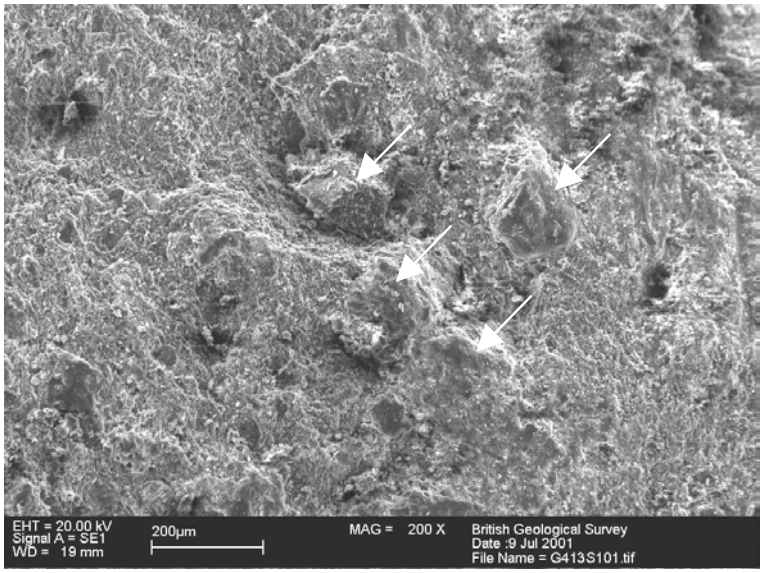

Plate 1. Massive mudrock, with several rounded fine-sand grade quartz grains (arrowed; sample G413, well 16/29-1, 2975 ft).

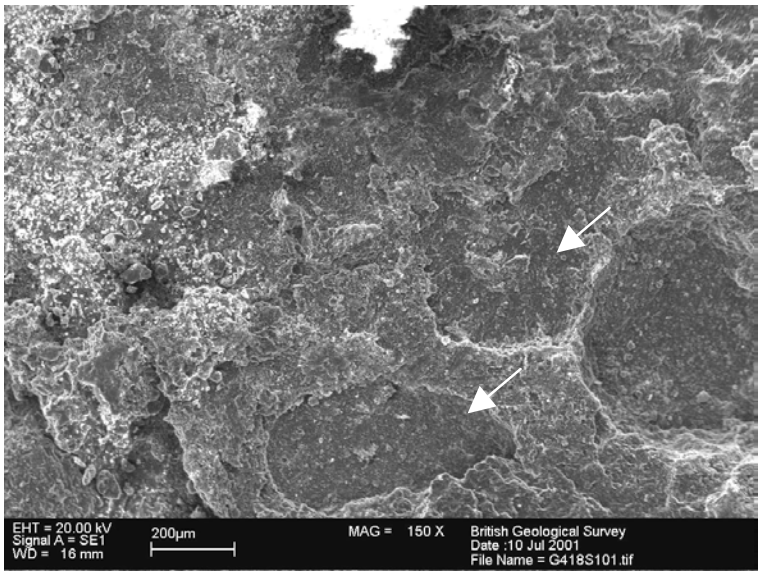

Plate 2. Massive mudrock with large (up to 0.5 mm) voids left where sand grains have been plucked out (arrowed; sample G418, well 16/28-3, 3248 ft).

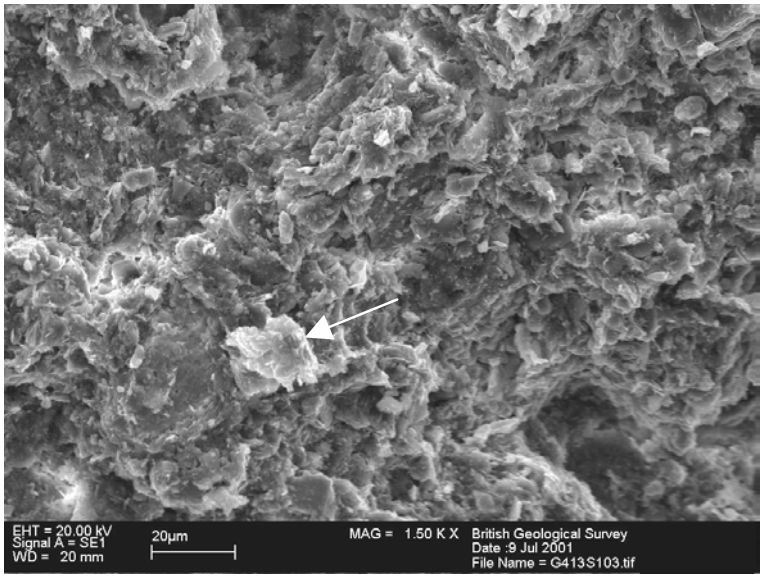

Plate 3. Detail of massive mudrock, showing tightly packed and essentially randomly oriented clay particles. Also note the presence of clay mineral particles up to c.20 µm in diameter (arrowed; sample G413, well 16/29-1, 2975 ft).

LAMINATED MUDROCKS

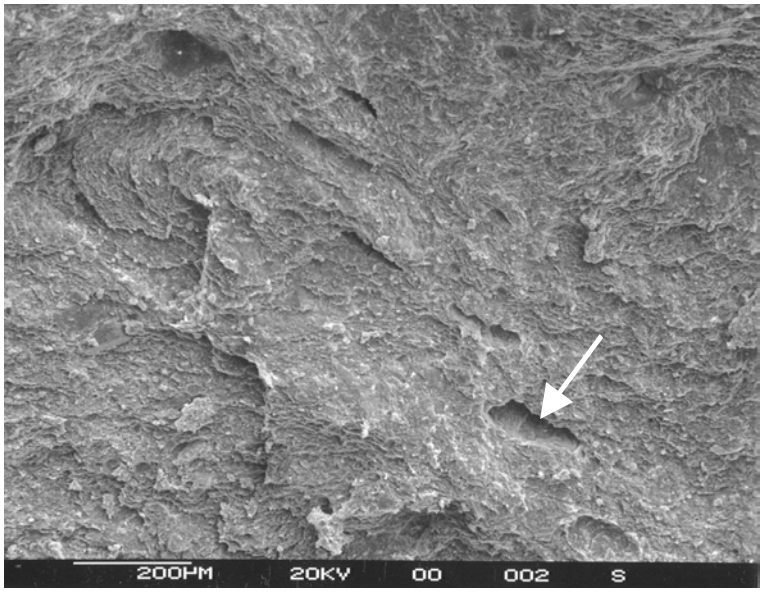

Plate 4. Laminated mudrock with holes where fine sand grade grains have been removed (arrowed; sample G421, well 16/29-4, 3463 ft).

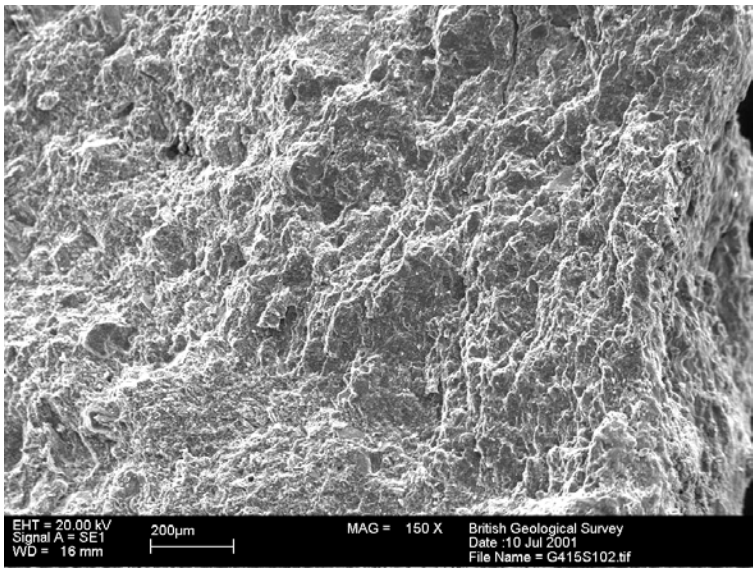

Plate 5. Laminated mudrock. The sample surface is at a low angle to the lamination which is defined by the terraced appearance of the sample (sample G415, well 16/29-1, 3275 ft).

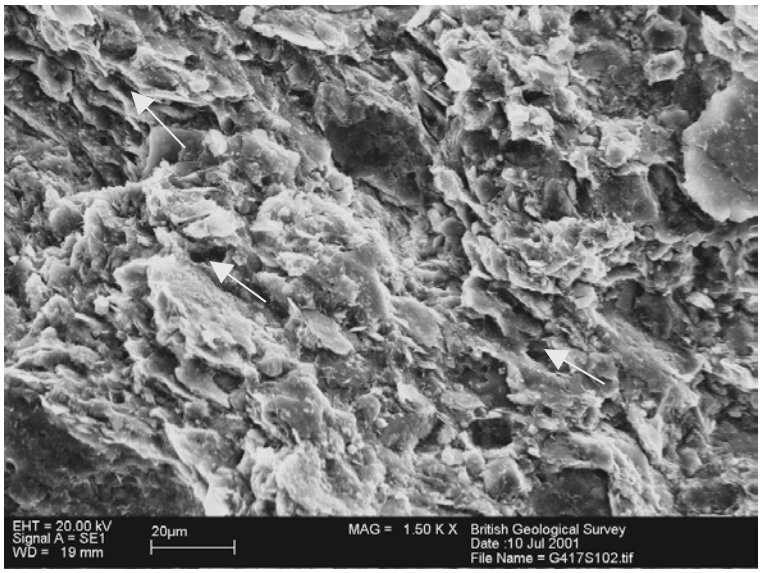

Plate 6. Detail of laminated mudrock showing tightly packed clay platelets, which display a preferred orientation. Micropores (arrowed) between clay particles are a few microns in diameter and poorly connected to each other. Also note the variation in clay mineral particle size (sample G417, well 16/28-3, 3183 ft).

SLICKENSIDES

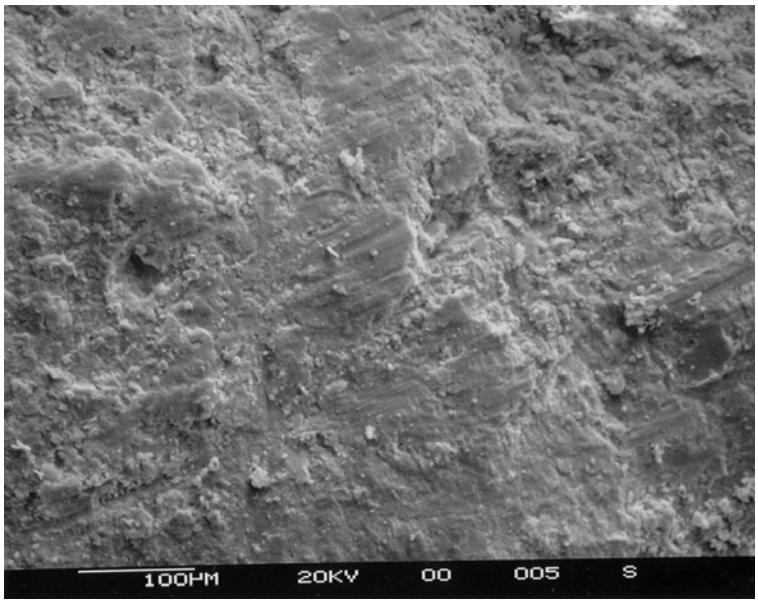

Plate 7. Mudrock with well developed slickensides (sample G410, well 16/28-5, 3609 ft).

SILT AND SAND-GRADE PARTICLES

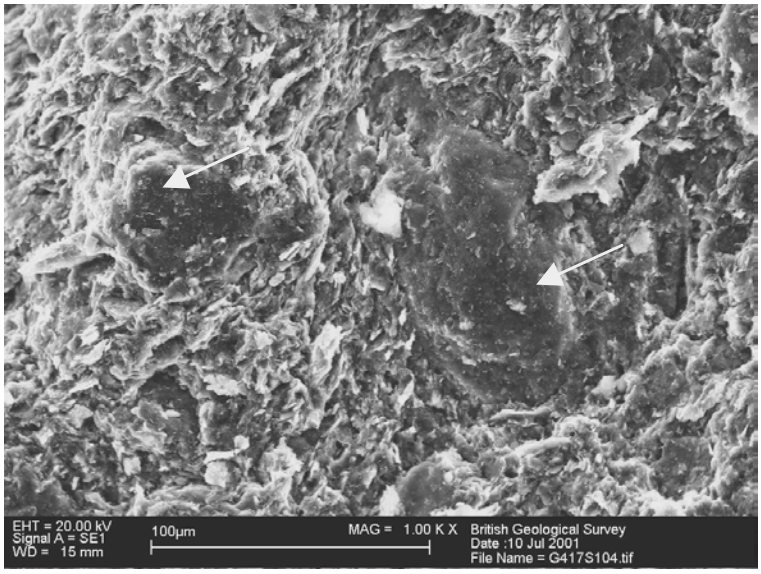

Plate 8. Well rounded, silt and fine sand grade quartz grains (arrowed) in a matrix of tightly packed clay particles, which are aligned around the margins of the grains (sample G417, well 16/28-3, 3183 ft).

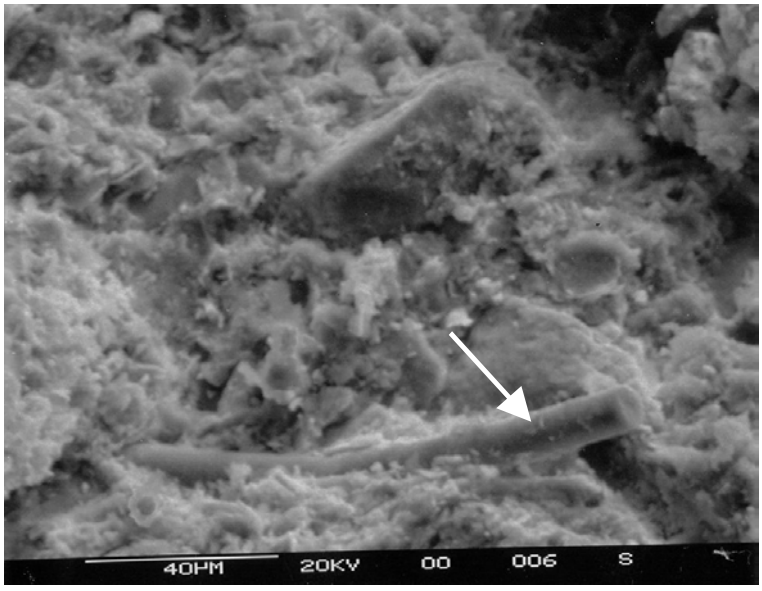

Plate 9. Elongate sponge spicule fragment (arrowed), and rounded silt-grade quartz grain (sample G410, well 16/28-5, 3609 ft).

DIAGENETIC PHASES

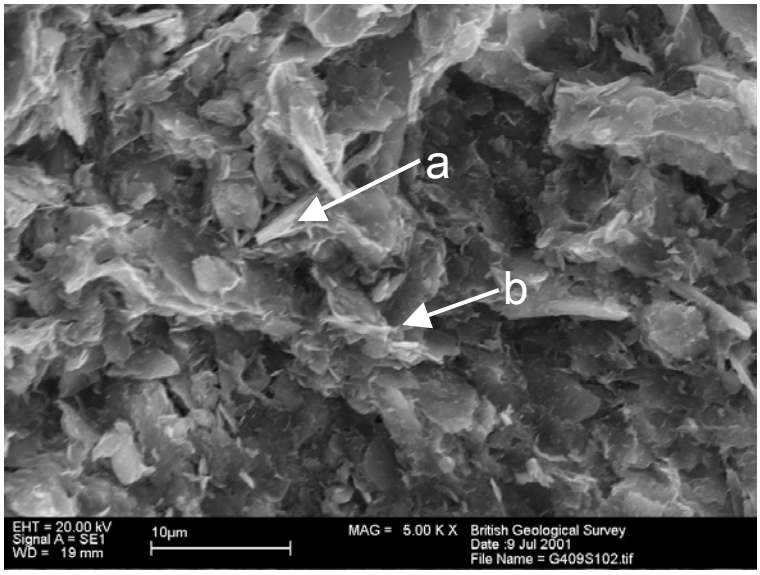

Plate 10. Clay particles displaying evidence for recrystallisation/ neomorphism, with the development of platey (arrowed, a) and fibrous crystals (arrowed b). This field of view displays relatively well developed micropores, up to a few microns in diameter between the clay particles (sample G409, well 16/29-2, 3125-3150 ft).

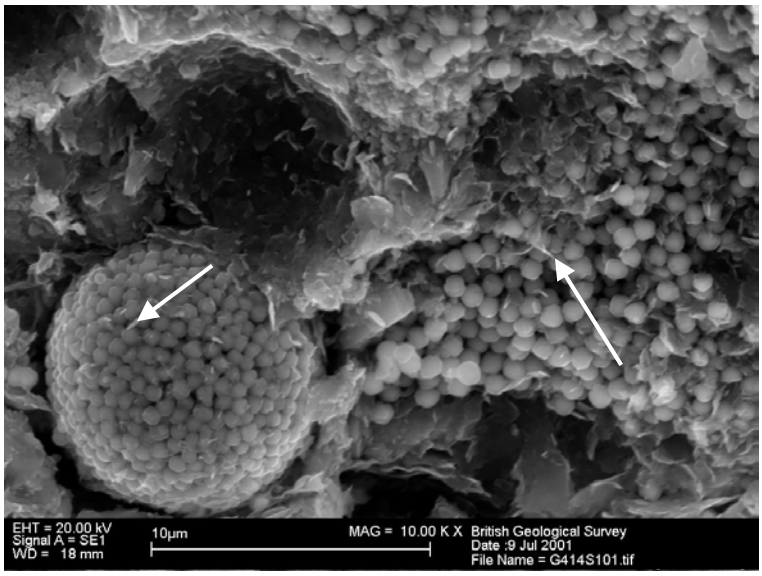

Plate 11. Detail of authigenic pyrite framboid, and disseminated pyrite crystals associated with finely crystalline authigenic(?) clay (arrowed; sample G414, well 16/29-1, 3125 ft).

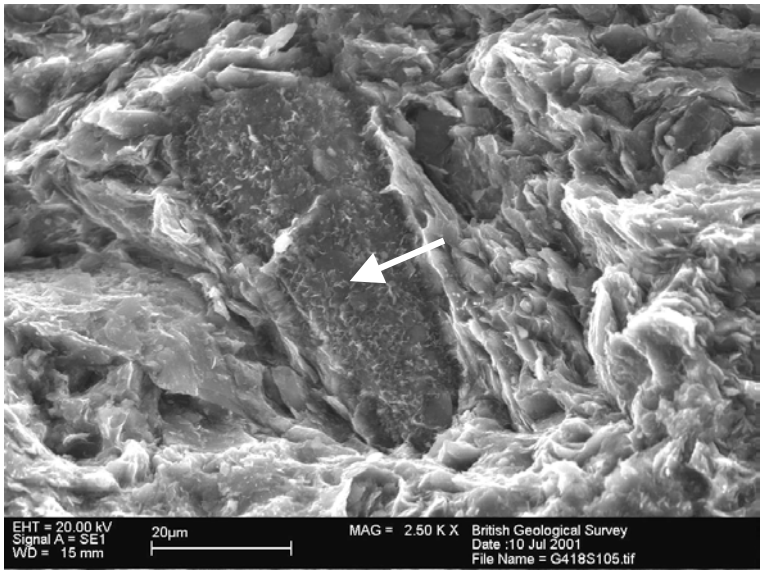

Plate 12. Detrital feldspar showing evidence for marginal illitisation (arrowed). Clay particles are relatively tightly packed with very minor amounts of sub-micron sized micropores (sample G418, well 16/28-3, 3248 ft).

INDUCED MICROFRACTURE

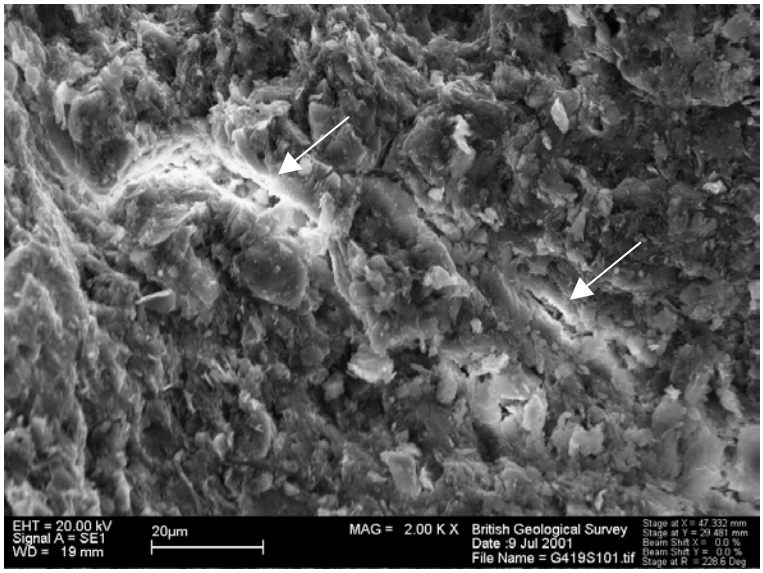

Plate 13. Microfracture (arrowed), interpreted to be the result of sample shrinkage during drying out (sample G419, well 16/23-1, 3100 ft).

HALITE/SYLVITE CONTAMINATION

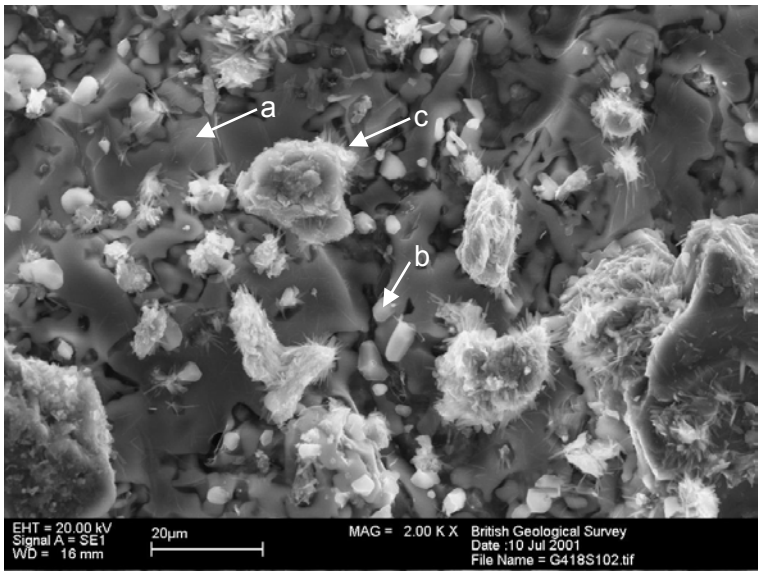

Plate 14. Halite (arrowed a) and sylvite (arrowed b) surface contamination. Also evident are clusters of illite platelets with fibrous, authigenic outgrowths (arrowed, c; sample G418, well 16/28-3, 3248 ft).

Appendix - Example X-ray diffraction traces

Three samples (16/08-1 2250 ft, 16/28-3 3248 ft and 16/28-5 3839 ft) are shown to illustrate the typical XRD traces produced by the Nordland Shale samples. In each case, a whole-rock trace is shown uppermost with the <2 μm fraction oriented mount traces below (air-dry; black trace, glycol-solvated; red trace, heated 550°C/2 hours; green trace). Horizontal scales show °2θ Co-Kα while vertical scales show intensity in counts/second. For the whole-rock traces, diagnostic peaks are labelled for each identified mineral phase including its d spacing (Å). All peaks are labelled for the <2 μm fraction glycol-solvated traces including the miller index (00*l*) for the clay minerals.

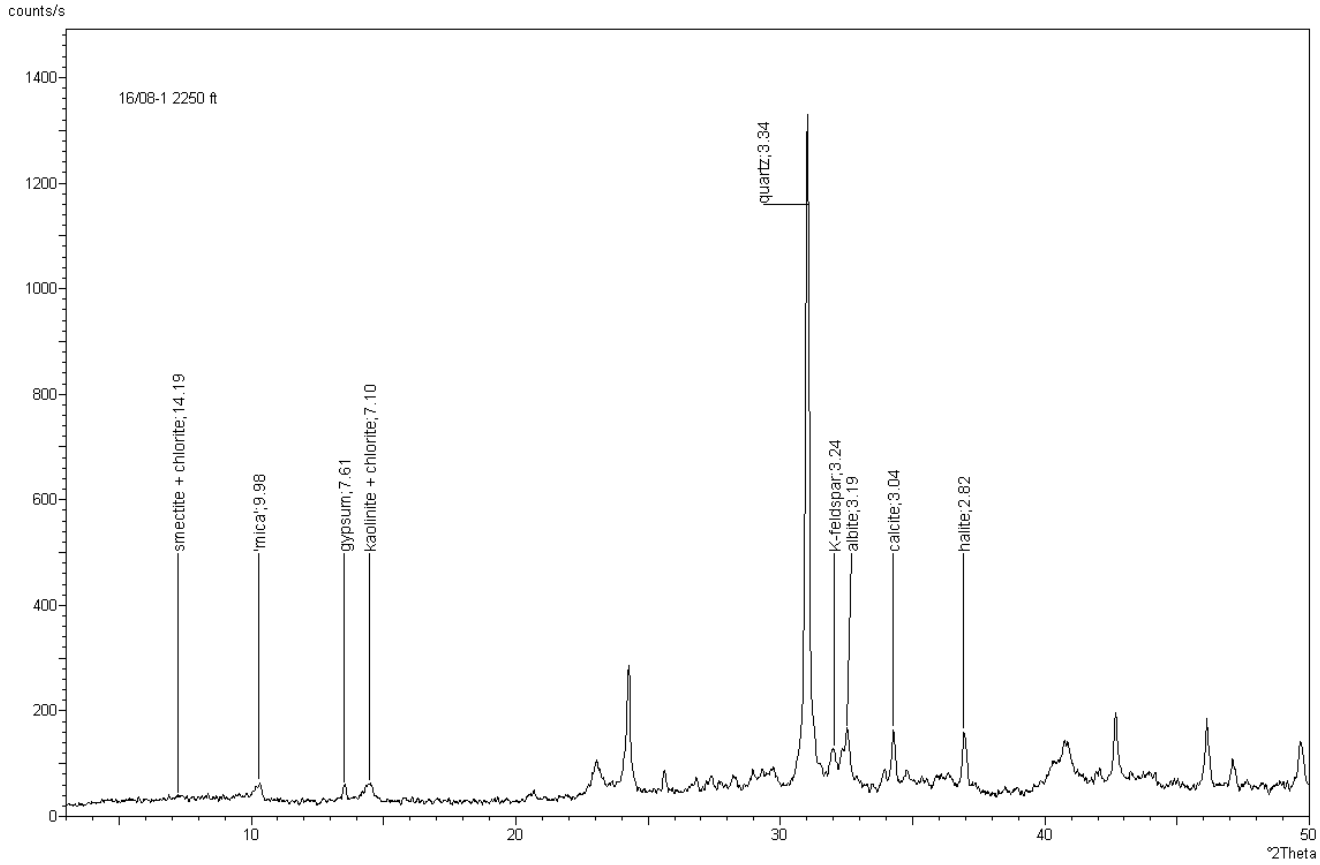
counts/s
16/08-1 2250 ft
smectite + chlorite;14.19
mica;9.98
gypsum;7.61
kaolinite + chlorite;7.10
quartz;3.34
K-feldspar;3.24
albite;3.19
calcite;3.04
halite;2.82
°2Theta

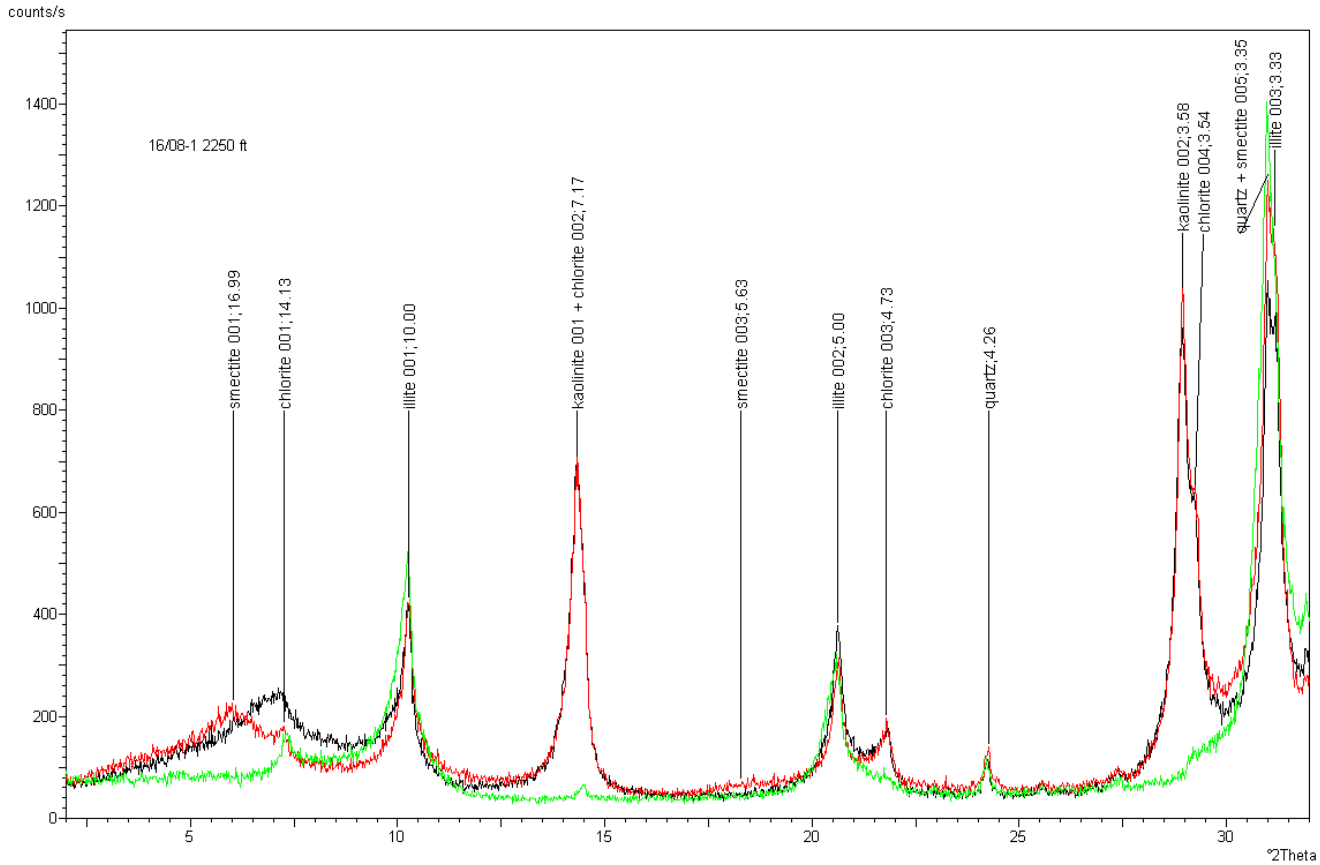
counts/s
16/08-1 2250 ft
smectite 001;16.99
chlorite 001;14.13
illite 001;10.00
kaolinite 001 + chlorite 002;7.17
smectite 003;5.63
illite 002;5.00
chlorite 003;4.73
quartz;4.26
kaolinite 002;3.58
chlorite 004;3.54
quartz + smectite 005;3.35
illite 003;3.33
°2Theta

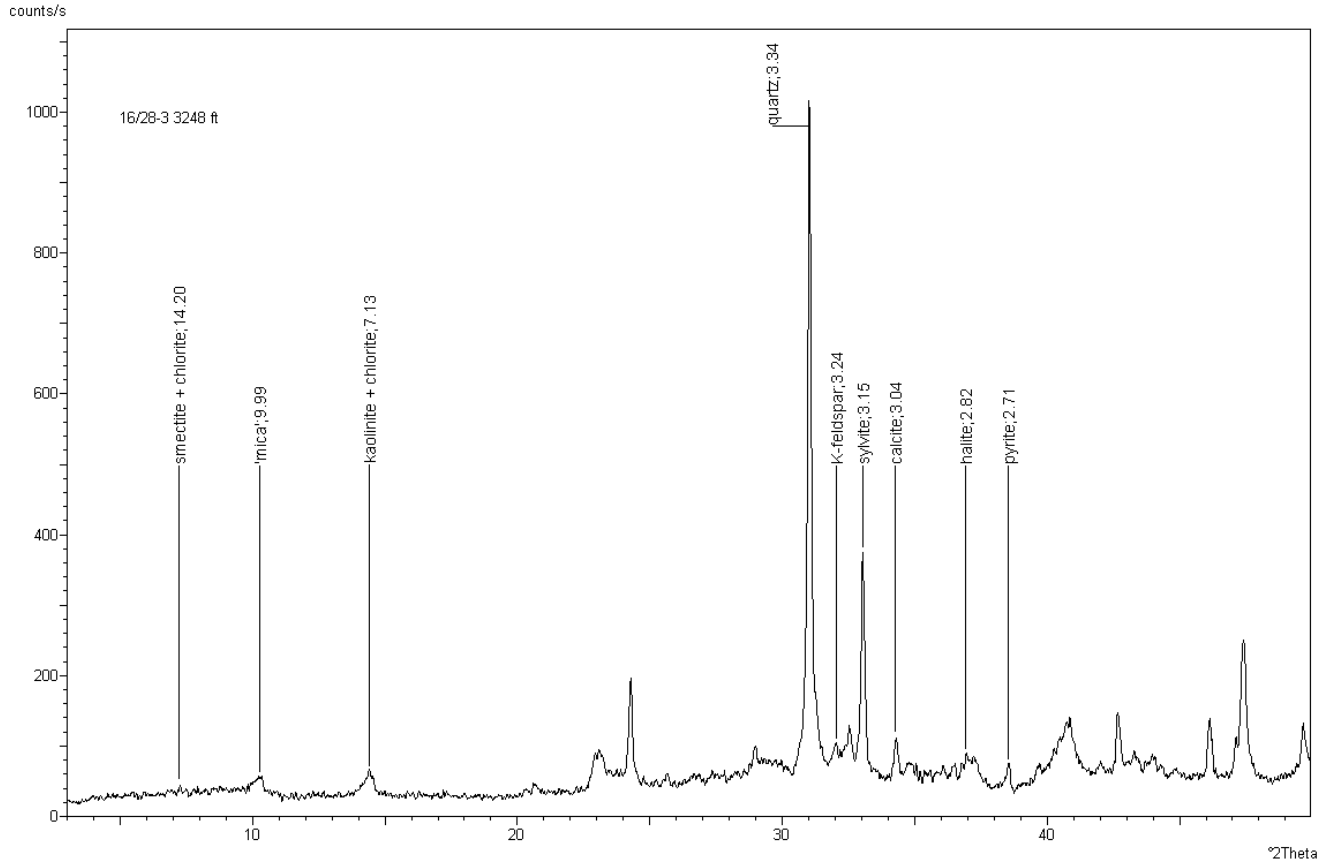
counts/s
16/28-3 3248 ft
quartz;3.34
smectite + chlorite;14.20
mica;9.99
kaolinite + chlorite;7.13
K-feldspar;3.24
sylvite;3.15
calcite;3.04
halite;2.82
pyrite;2.71
°2Theta

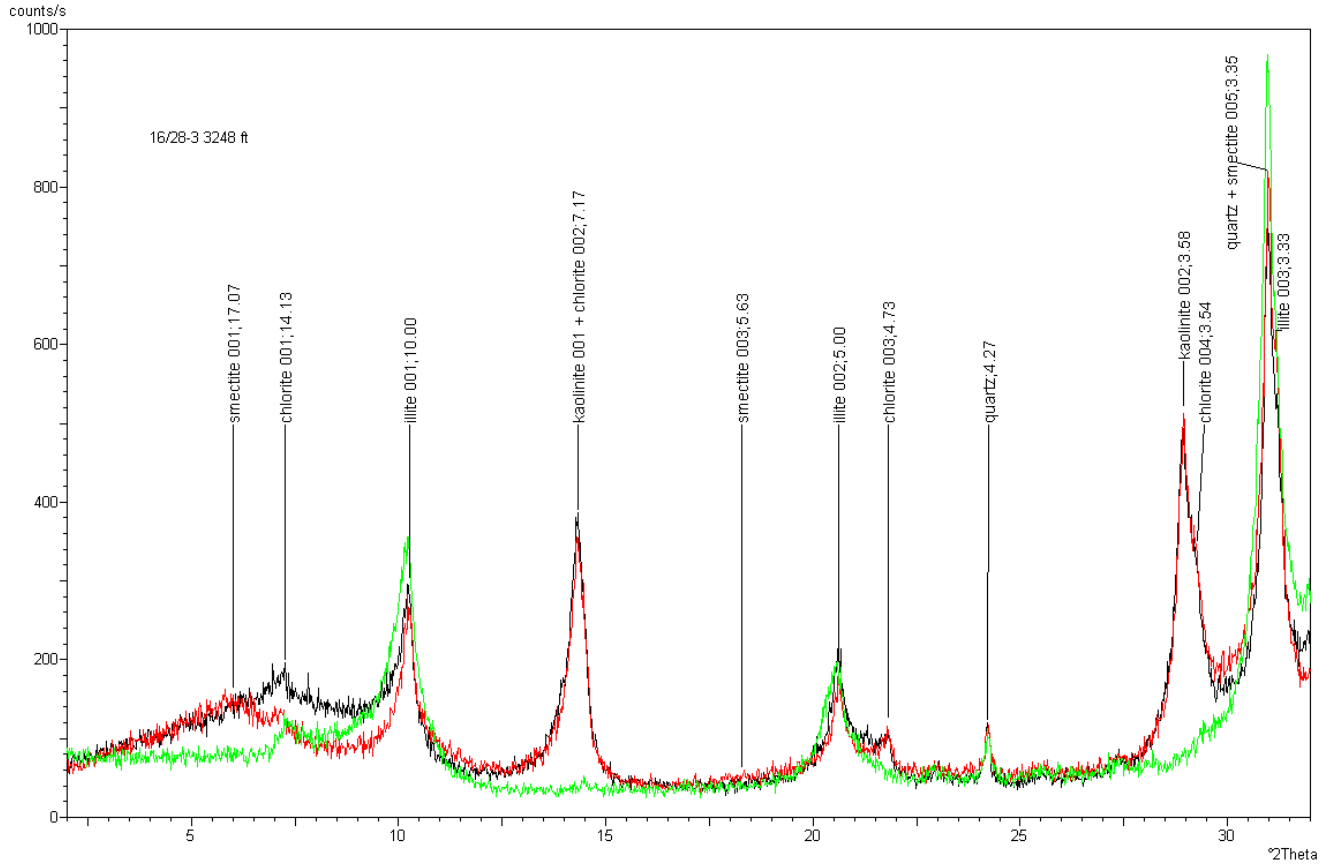
counts/s
16/28-3 3248 ft
smectite 001;17.07
chlorite 001;14.13
illite 001;10.00
kaolinite 001 + chlorite 002;7.17
smectite 003;5.63
illite 002;5.00
chlorite 003;4.73
quartz;4.27
kaolinite 002;3.58
chlorite 004;3.54
quartz + smectite 005;3.35
illite 003;3.33
°2Theta

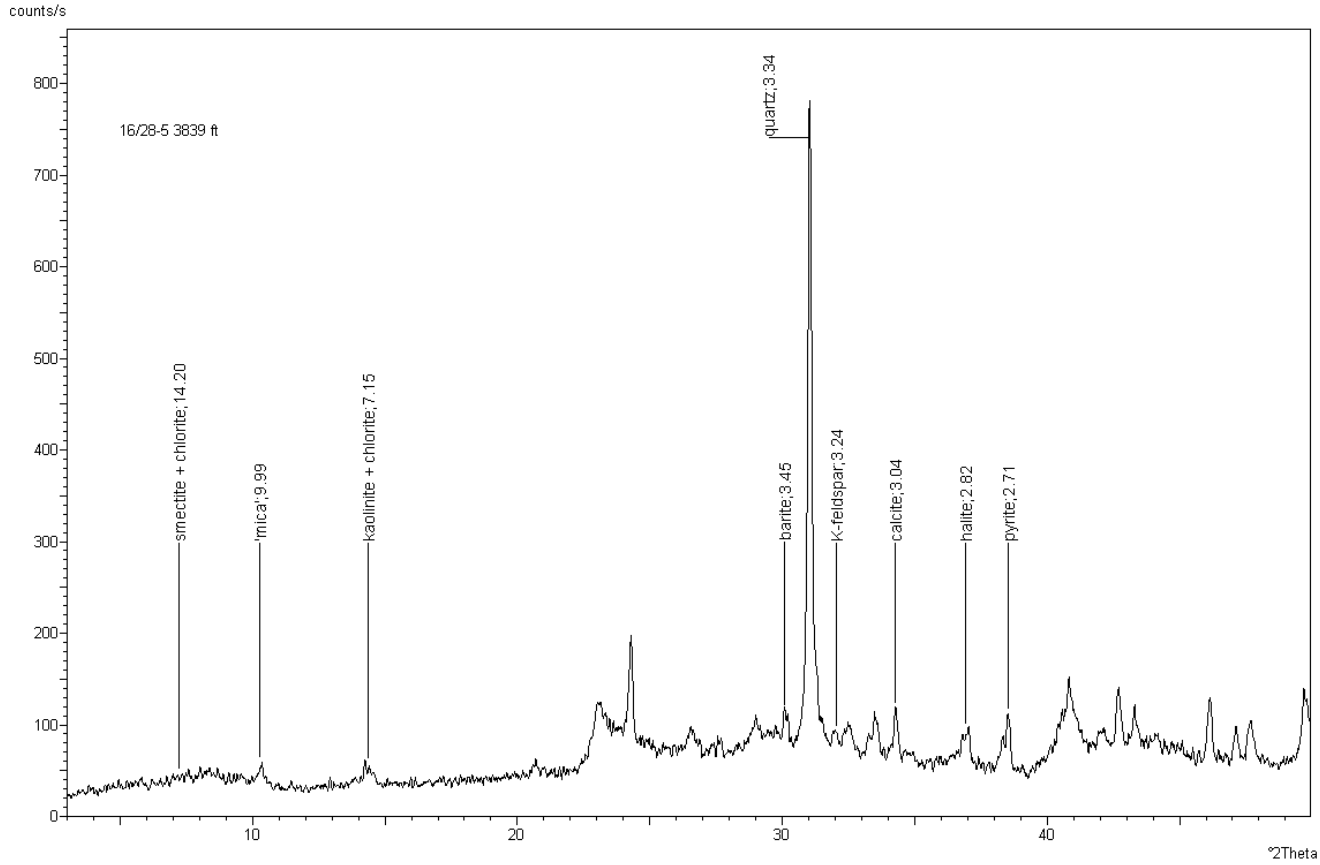
counts/s
16/28-5 3839 ft
quartz;3.34
smectite + chlorite;14.20
mica;9.99
kaolinite + chlorite;7.15
barite;3.45
K-feldspar;3.24
calcite;3.04
halite;2.82
pyrite;2.71
°2Theta

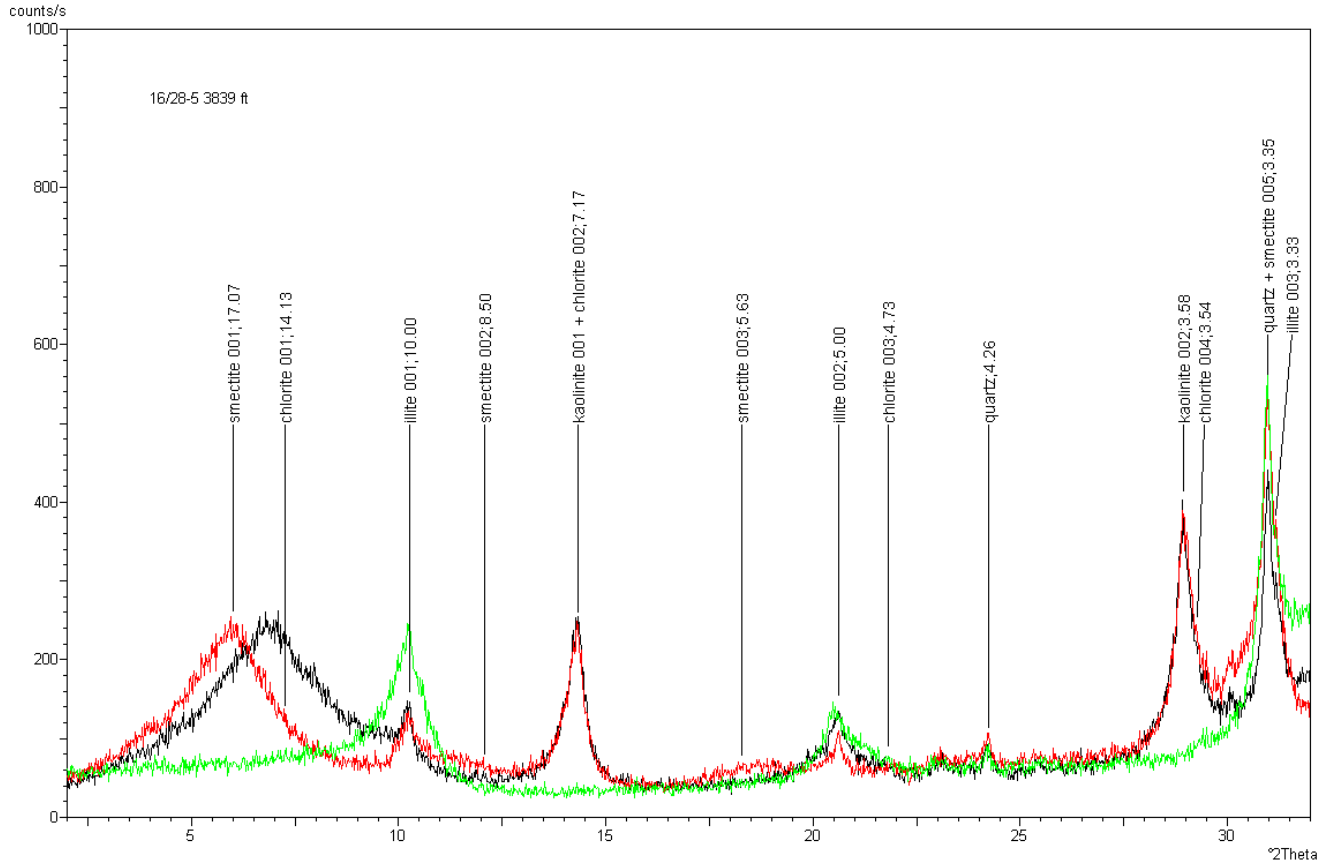
counts/s
16/28-5 3839 ft
smectite 001;17.07
chlorite 001;14.13
illite 001;10.00
smectite 002;8.50
kaolinite 001 + chlorite 002;7.17
smectite 003;5.63
illite 002;5.00
chlorite 003;4.73
quartz;4.26
kaolinite 002;3.58
chlorite 004;3.54
quartz + smectite 005;3.35
illite 003;3.33
°2Theta